Chapter 5

GEOCHEMISTRY

Prior to the South Mountain Batholith project there were numerous geochemical studies of the South Mountain Batholith including Smith (1974), McKenzie and Clarke (1975), Smith (1979), Muecke and Clarke (1981), Chatterjee and Muecke (1982), Chatterjee and Strong (1984a,b), Clarke and Muecke (1985), Clarke and Chatterjee (1988). In general these studies involved either small sample populations (i.e. $<$ca. N=30) that were used to characterize the compositions of the major rock types in the batholith or larger sample suites (e.g. ca. N=100-200) that were collected in localized areas of the batholith. A large number of samples (N=597) were collected and analyzed for a suite of major and trace elements as part of the South Mountain Batholith project. The main aims were to define the complete compositional range for each of the rock types in the sundry plutons, defined during mapping, and to determine if any spatial compositional trends (i.e. zoning) could be delineated. The following sections outline: the sampling and analytical methods used in the South Mountain Batholith project; the geochemical characteristics of the major rock types in the batholith; the nature of chemical zoning in both Stage I and II plutons; and the geochemistry of leucogranite, mafic porphyry and dyke rocks.

5.1 Methodology

A total of 597 large (approximately 25 kg) samples from the entire batholith were chosen for major and trace element chemical analysis. Wherever possible, samples were collected from blasted roadside outcrop. In more remote areas, mainly along secondary and bush roads, it was necessary to drill and blast outcrop to acquire "fresh" or unweathered material for analysis. Two

sample suites were collected: 1) representative samples of the seven major rock types which were selected on the basis of results of systematic geological mapping, investigation of stained slabs, detailed petrography and outcrop distribution; and 2) samples of aplite, mineralized and barren pegmatite dykes, alteration zones and mineralized greisens, veins and breccias.

Whenever possible, a minimum of 25 kg of material was collected from large outcrop areas to eliminate potential problems of heterogeneity. Clearly, for some of the dykes and mineralized zones this was not possible and much smaller samples were collected. Samples were then crushed to minus 2.5 cm, homogenized and then approximately 4 kg of fresh material was handpicked to eliminate weathering, fracture-related alteration and xenoliths. The hand-picked material was then ultrasonically cleaned, dried, crushed to minus 5 mm and split to form a 200 gm subsample which was subsequently crushed in a ceramic shatter box to minus 200 mesh.

Bench standards were prepared for quality control in the analytical procedures. Standard NIC-1 is a medium grained, non megacrystic biotite granodiorite which was collected in a rock quarry in a satellite intrusion north of the batholith, near Nictaux (MacDonald and Ham, 1992). Standard ASPO-2 is a sample of the Sandy Lake biotite monzogranite (Corey, 1990) which was collected along Highway #103, north of the Aspotogan peninsula. Approximately 200 kg of fresh material was collected and crushed according to the above procedure. Mean values and standard deviations for trace and major element compositions for the two standards are presented in Table 5.1.

Samples, analytical splits and bench standards were sent to the Regional X-Ray fluorescence (XRF) facilities at St. Mary's University for analysis of major elements including SiO_2, TiO_2, Al_2O_3, Fe_2O_{3t}, MnO, MgO, CaO, Na_2O, K_2O and P_2O_5 and a suite of trace elements

(Ba, Rb, Sr, Y, Zr, Nb, Pb, Zn, Cu, Ni, V and Cr). Major element concentrations were determined using fused glass discs whereas pressed powder pellets were used for trace element determinations. The same suite of samples and standards were sent to Bondar-Clegg Laboratories for determination of 12 additional trace elements. Analytical procedures included: Instrumental Neutron Activation Analysis (INAA) for Sc, As, La, Hf, Ta, W, Th and U; Atomic Absorption (AA) for Li; Specific Ion Electrode for F; DC Plasma Emission Spectroscopy for B; and X-Ray fluorescence for Sn. Several sample subsets were sent to the analytical facility at Memorial University in Newfoundland for analysis of rare earth elements (REE). Samples were analyzed by Inductively Coupled Plasma Mass Spectrometry (ICP-MS) using a sodium peroxide (Na_2O_2) sinter digestion.

5.2 Results

5.2.1 Geochemistry of Major Rock Types

Complete analytical results, with the exception of REE results, are given in Ham et al. (1989, 1990). Average major and trace element compositions and normative mineralogy, with standard deviations, for the major rock types in the five Stage I and eight Stage II plutons are presented in Tables 5.1 and 5.2. Complete analytical results for individual plutons are given in Appendix A. The analytical errors are $\leq 2\%$ for the major elements and $\leq 10\%$ for most of the trace elements with the exception of Pb, Hf, Ta, La, Th and U where errors are $\leq 20\%$ of the reported values. A complete discussion of all geochemical characteristics for all samples analyzed during this project is beyond the scope of this report. Consequently the following section will focus on the average rock type compositions for Stage I and II plutons and also the compositional trends in selected plutons.

A significant geochemical parameter for granitic rocks is the Shand Index value which separates rocks into peraluminous, metaluminous and peralkaline groups. Average rock type compositions for Stage I and II plutons have been plotted on a Shand-type diagrams (Figs 5.1a,b). Clearly all of the rocks of the batholith are peraluminous (i.e. molecular $Al_2O_3/(CaO+K_2O+Na_2O) > 1$) with average A/CNK values ranging from 1.05 to 1.45. There is large overlap in the average A/CNK and A/NK values for the various rock types, however, it should be noted that the lowest average A/CNK values (1.05-1.10) are for mafic porphyry and biotite granodiorite units whereas the highest average values (1.40-1.45) are for muscovite leucogranites suggesting a relationship between "degree of differentiation" and alumina oversaturation. It should be also noted that these data contrast predicted results if the "restite unmixing" process of Chappell and White (1974) and White et al. (1986) is employed to explain chemical changes in the batholith. That is, the rocks with the highest proportion of metasedimentary xenoliths (restite) should have the highest A/CNK values. It should also be noted that all rocks of the batholith have relatively high SiO_2 and low CaO, when compared to other worldwide granite massifs, with average concentrations ranging from 67.12% (SD-1.73) and 1.94% (SD-0.46), respectively, in granodiorite to 73.62% (SD-0.89) and 0.39 (SD-0.14), respectively, in leucogranite rocks.

Several overall major element "trends" have been previously been noted in both Stage I and II plutons (MacDonald and Horne, 1988; Chatterjee and Horne, 1991; MacDonald et al., 1992). To demonstrate this feature, Harker variation diagrams have been prepared for the five Stage I and eight Stage II plutons (Figs 5.2a,e and 5.3a,h).

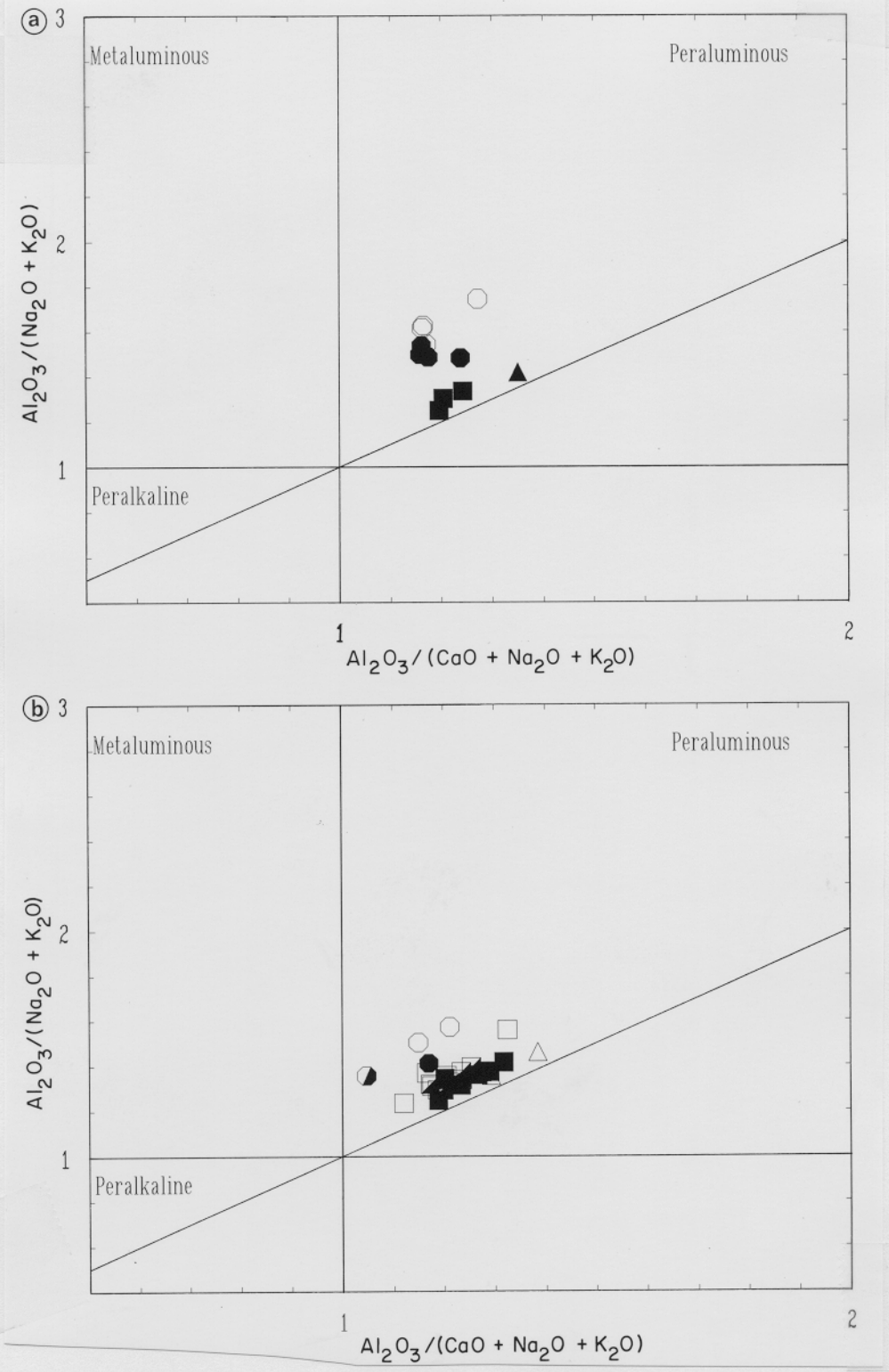

Figure 5.1 Plot of average A/CNK (i.e. molecular $Al_2O_3/(CaO+K_2O+Na_2O) > 1$) versus A/NK for the major rock types of the South Mountain Batholith (after Shand, 1931). a) Stage I plutons; b) Stage II plutons. All rocks are peraluminous.

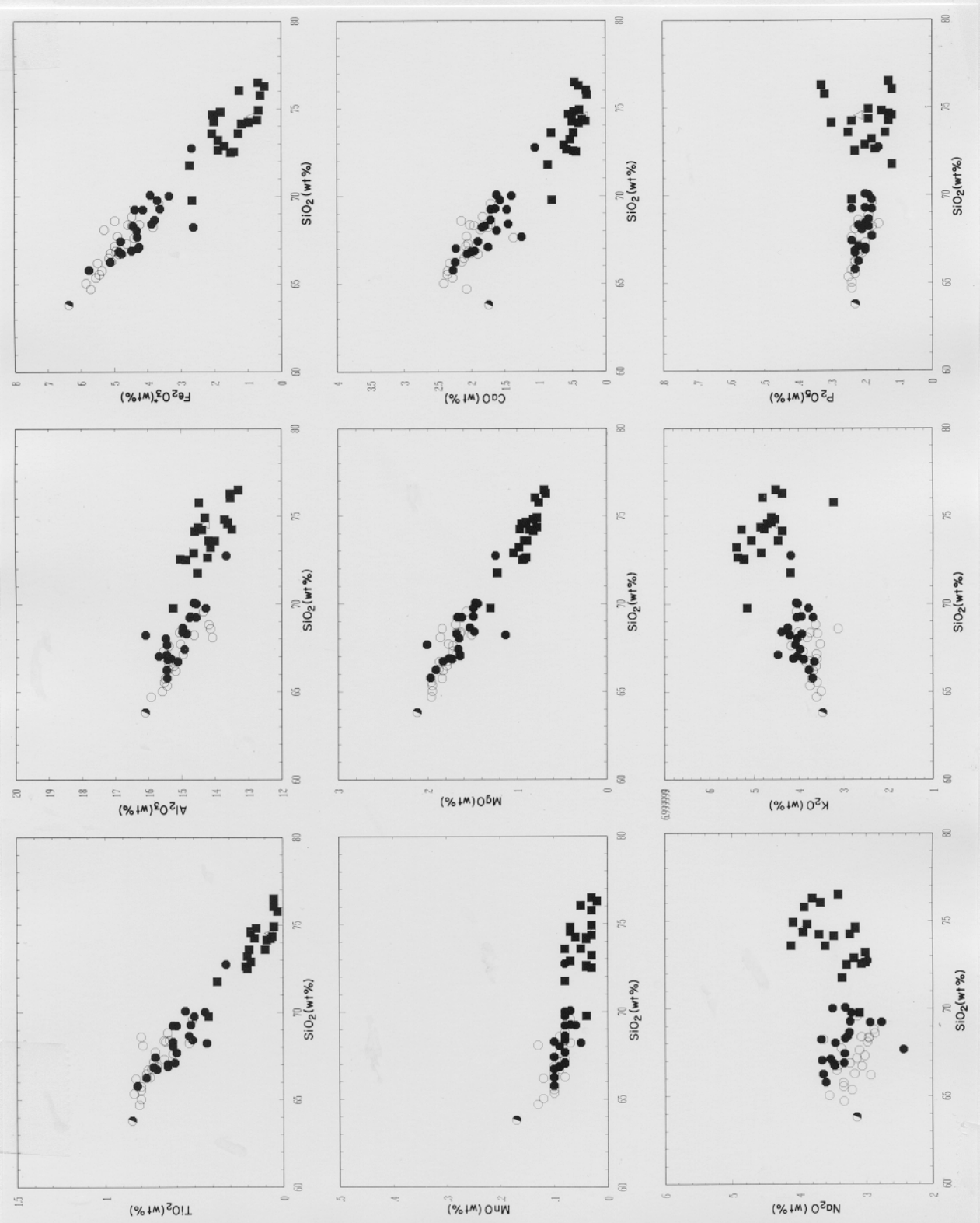

Figure 5.2a Harker variation diagrams for the Scrag Lake Stage I pluton.

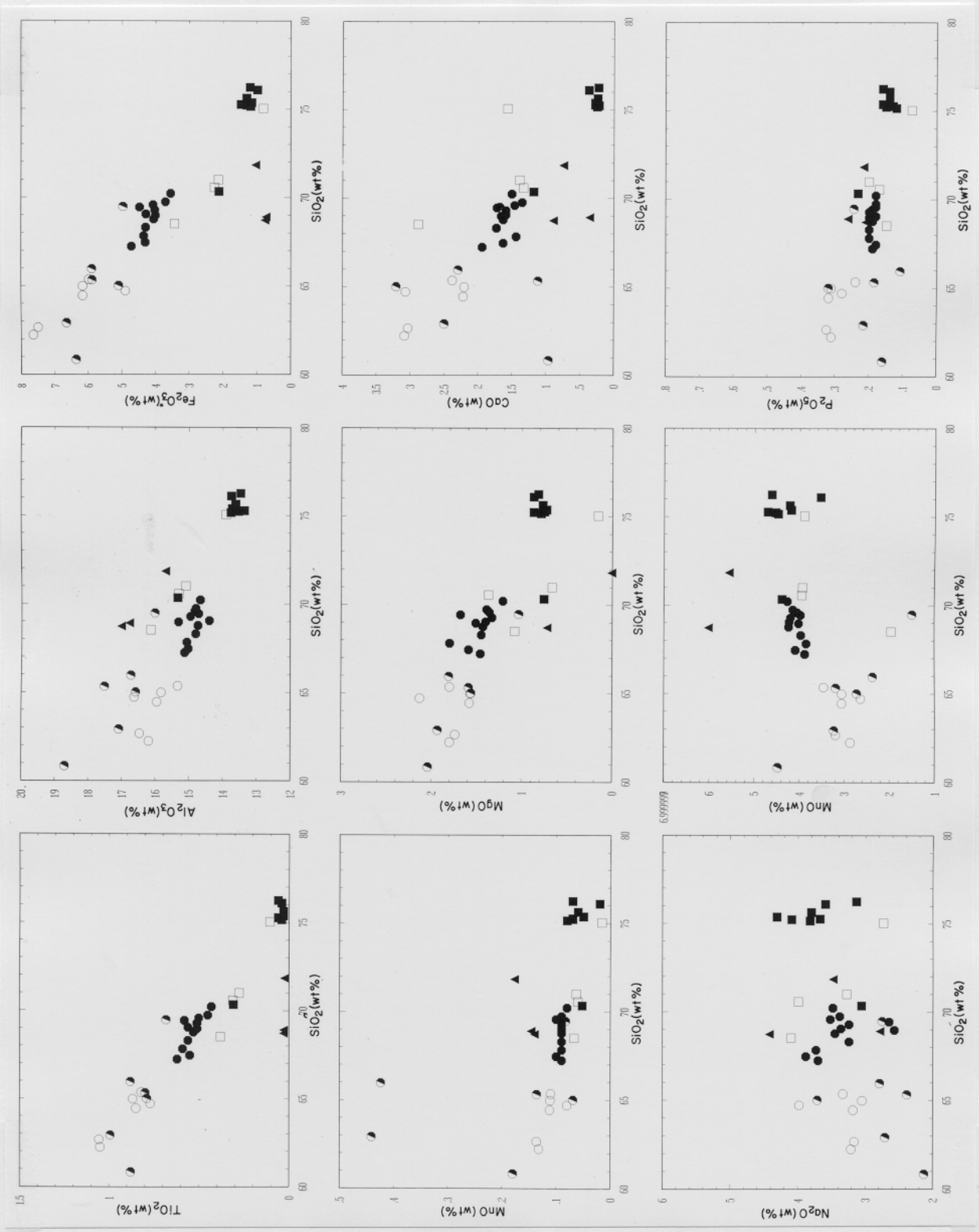

Figure 5.2b Harker variation diagrams for the Cloud Lake Stage I pluton.

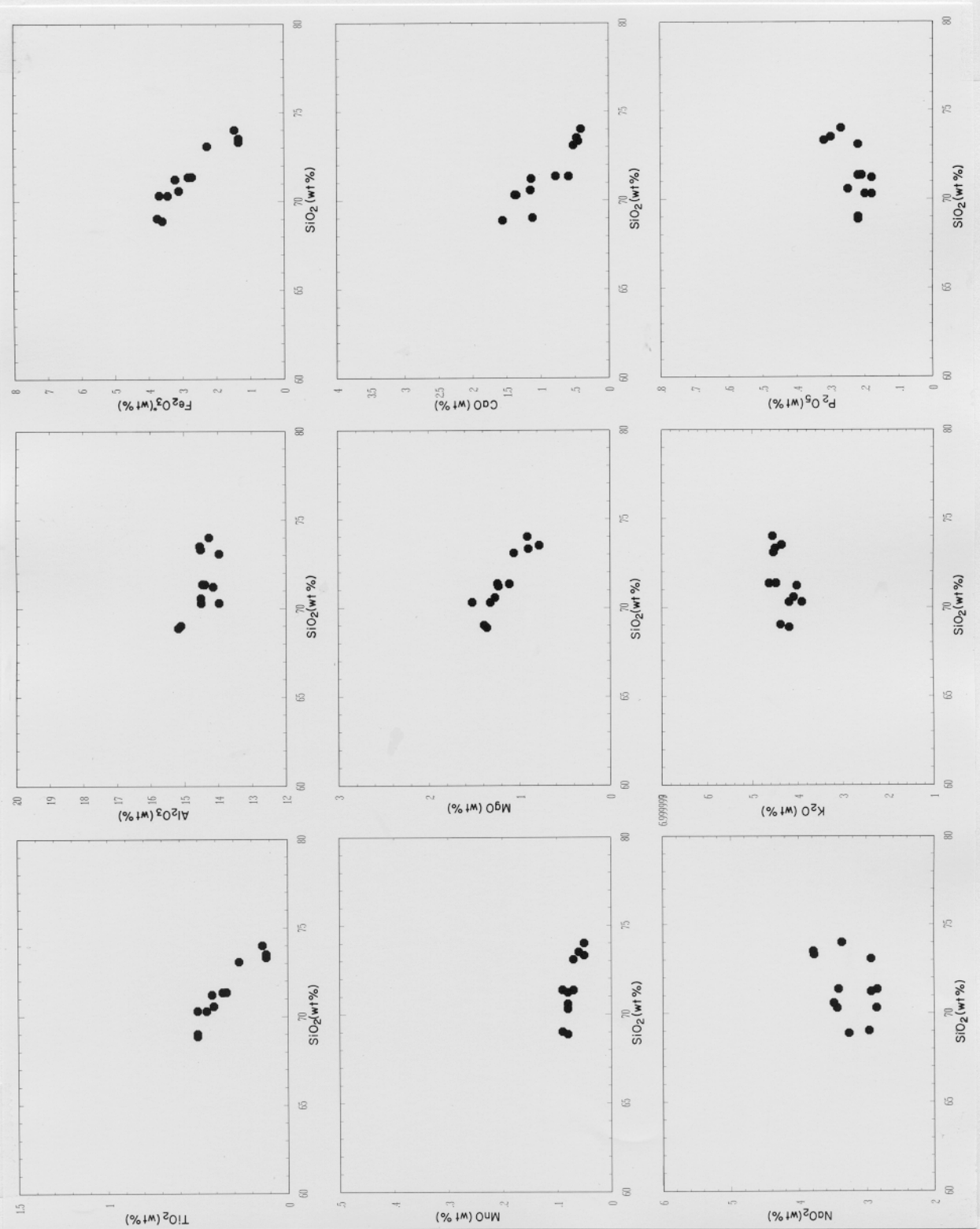

Figure 5.2c Harker variation diagrams for the Little Round Lake Stage I pluton.

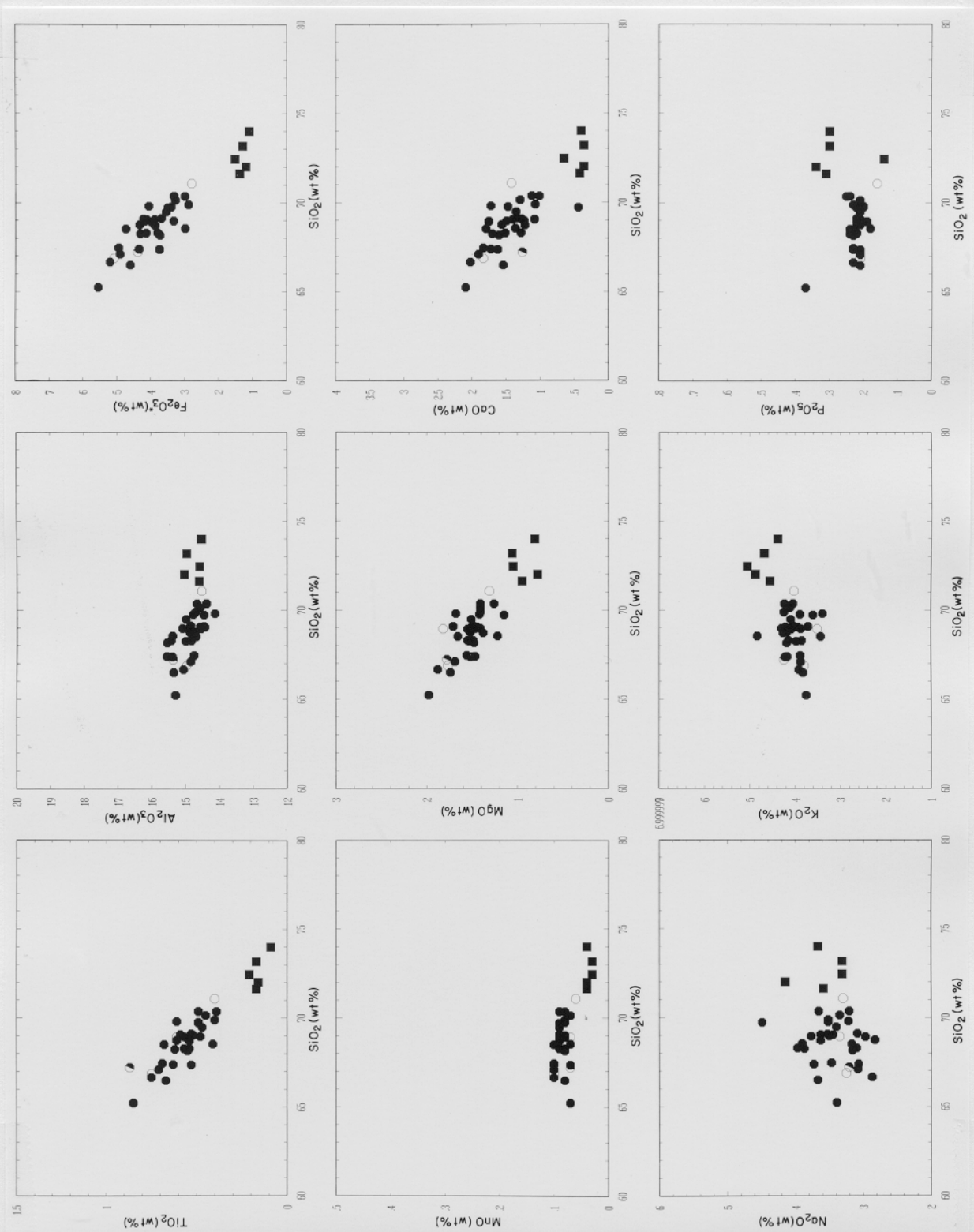

Figure 5.2d Harker variation diagrams for the Salmontail Lake Stage I pluton.

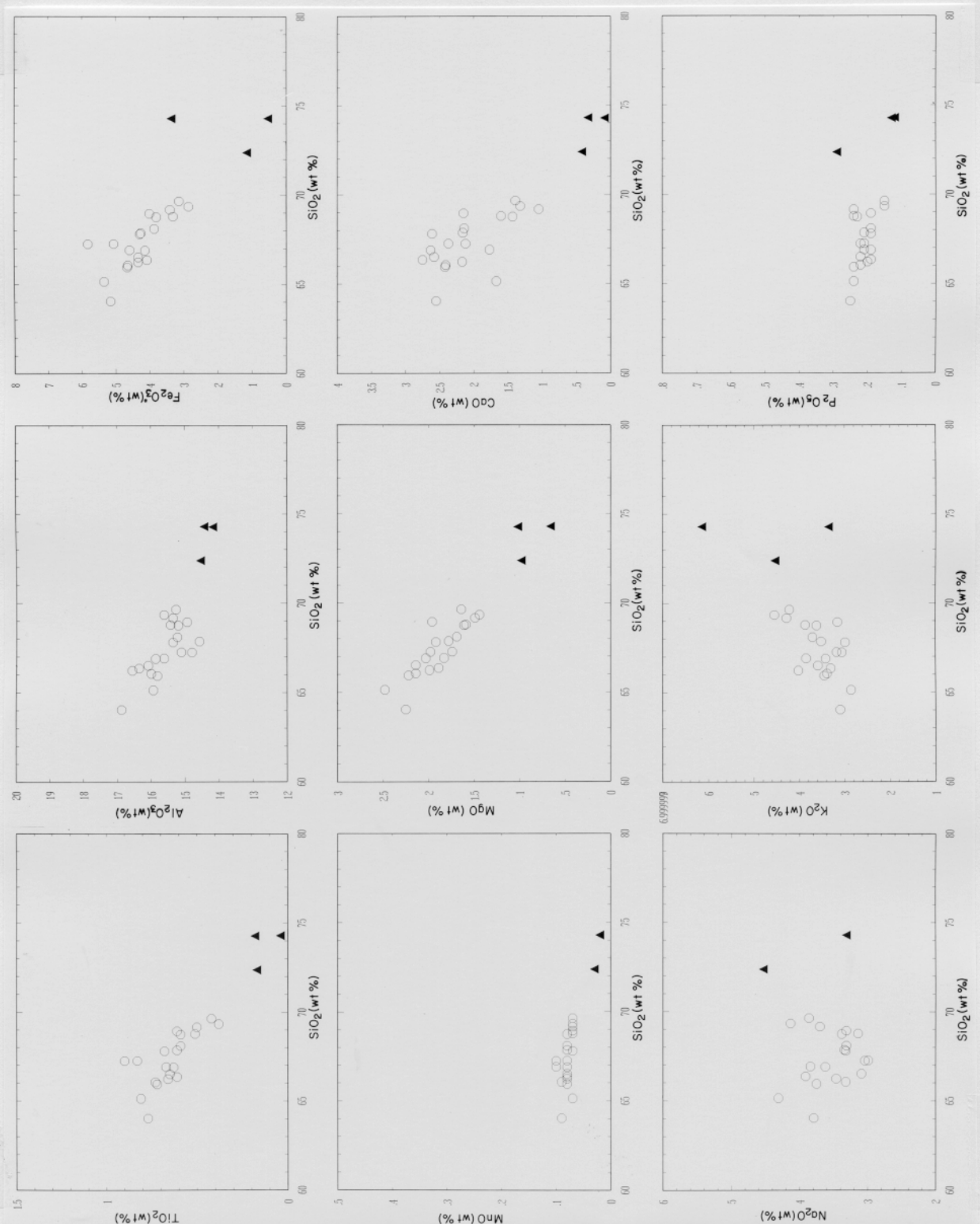

Figure 5.2e Harker variation diagrams for the Five Island Lake Stage I pluton.

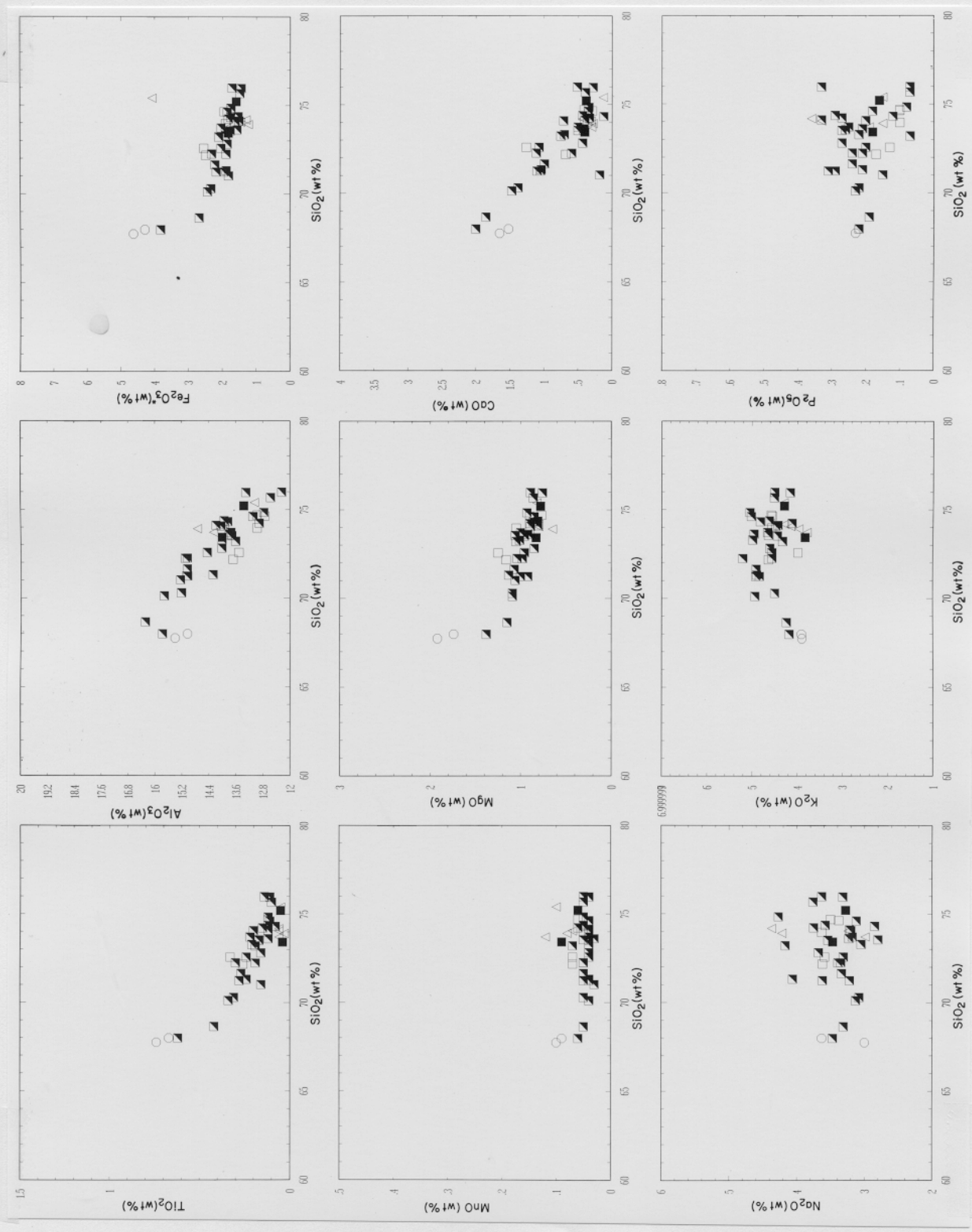

Figure 5.3a Harker variation diagrams for the Davis Lake Stage II pluton.

Figure 5.3b Harker variation diagrams for the Kejimkujik Stage II pluton.

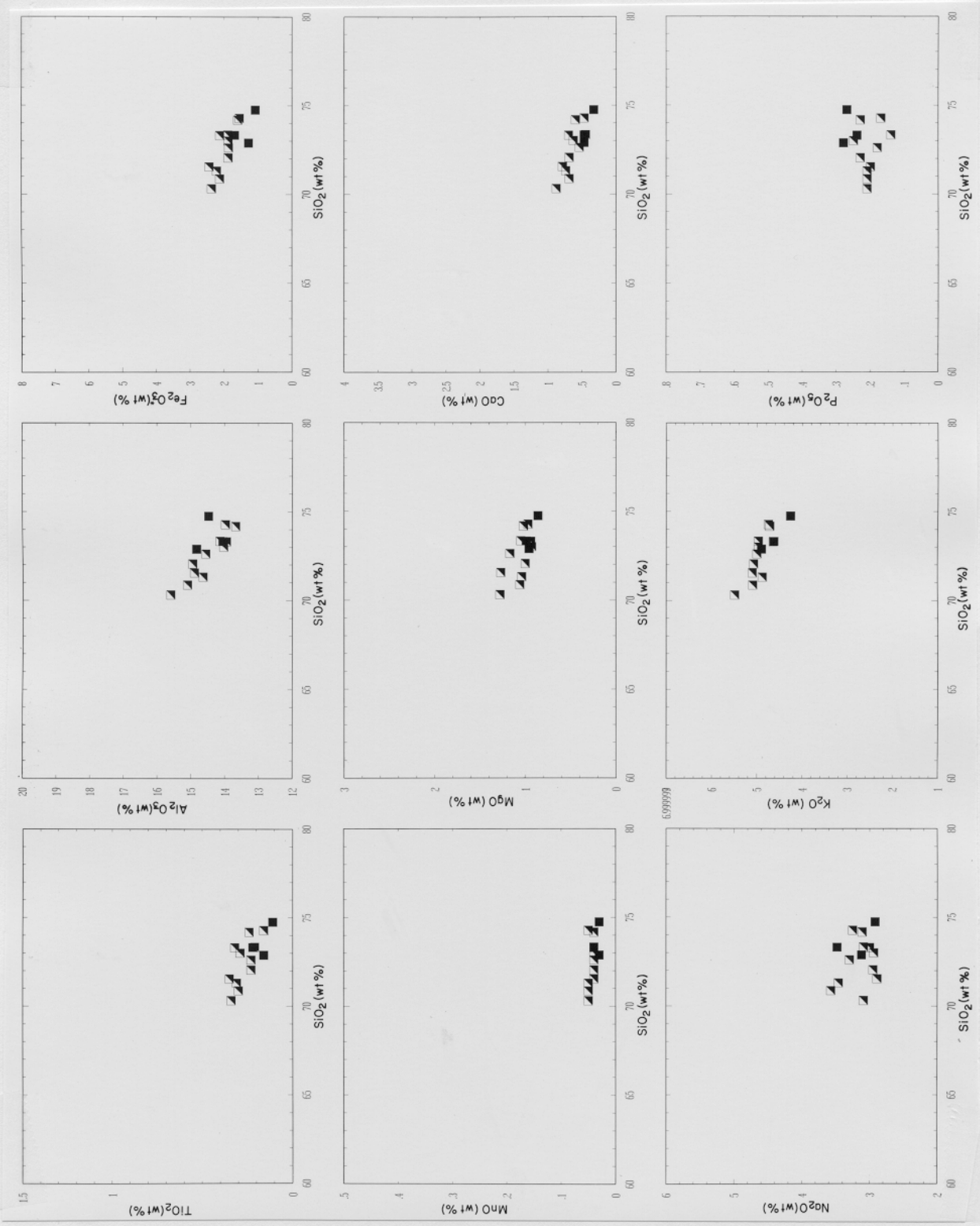

Figure 5.3c Harker variation diagrams for the West Dalhousie Stage II pluton.

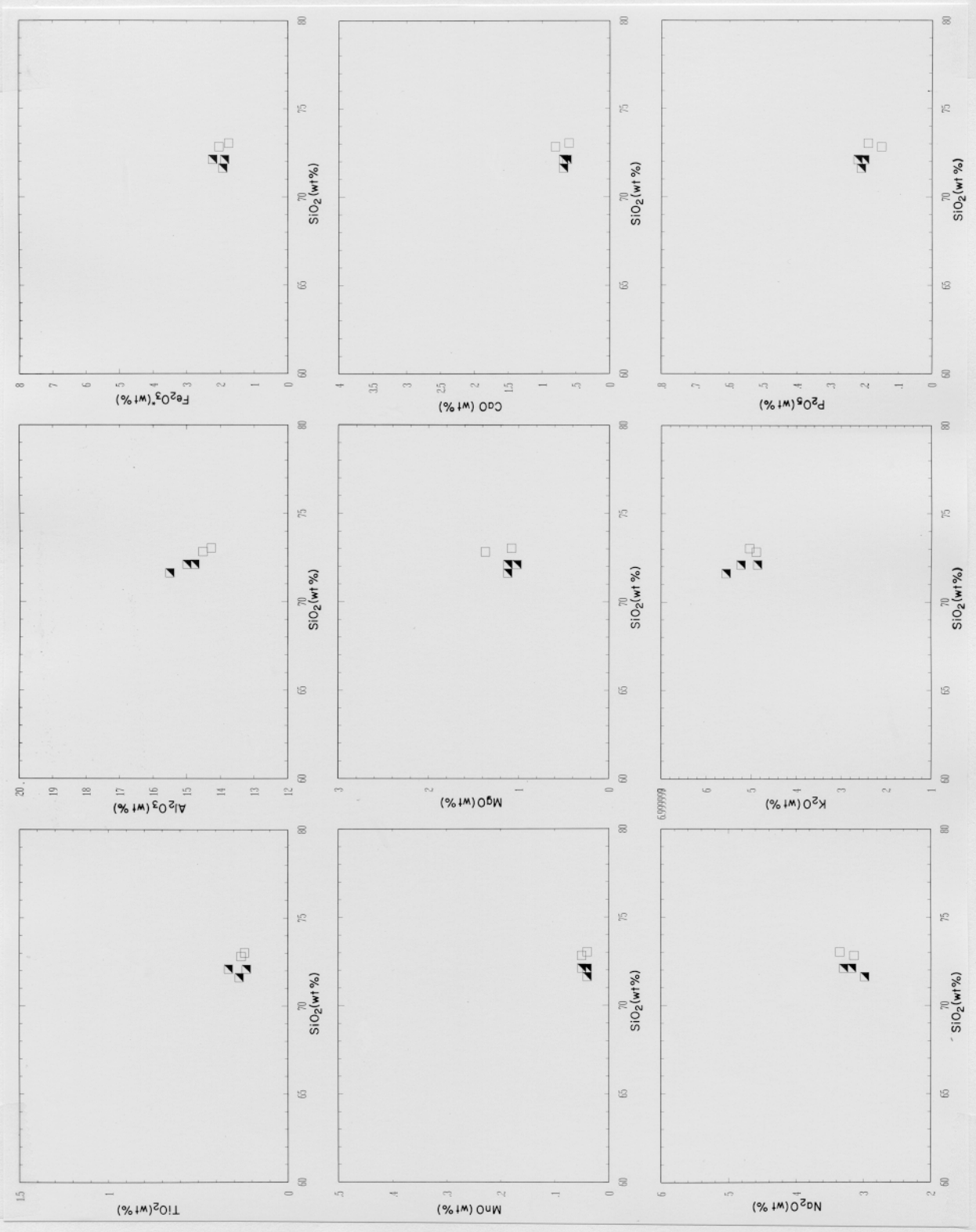

Figure 5.3d Harker variation diagrams for the Morse Road Stage II pluton.

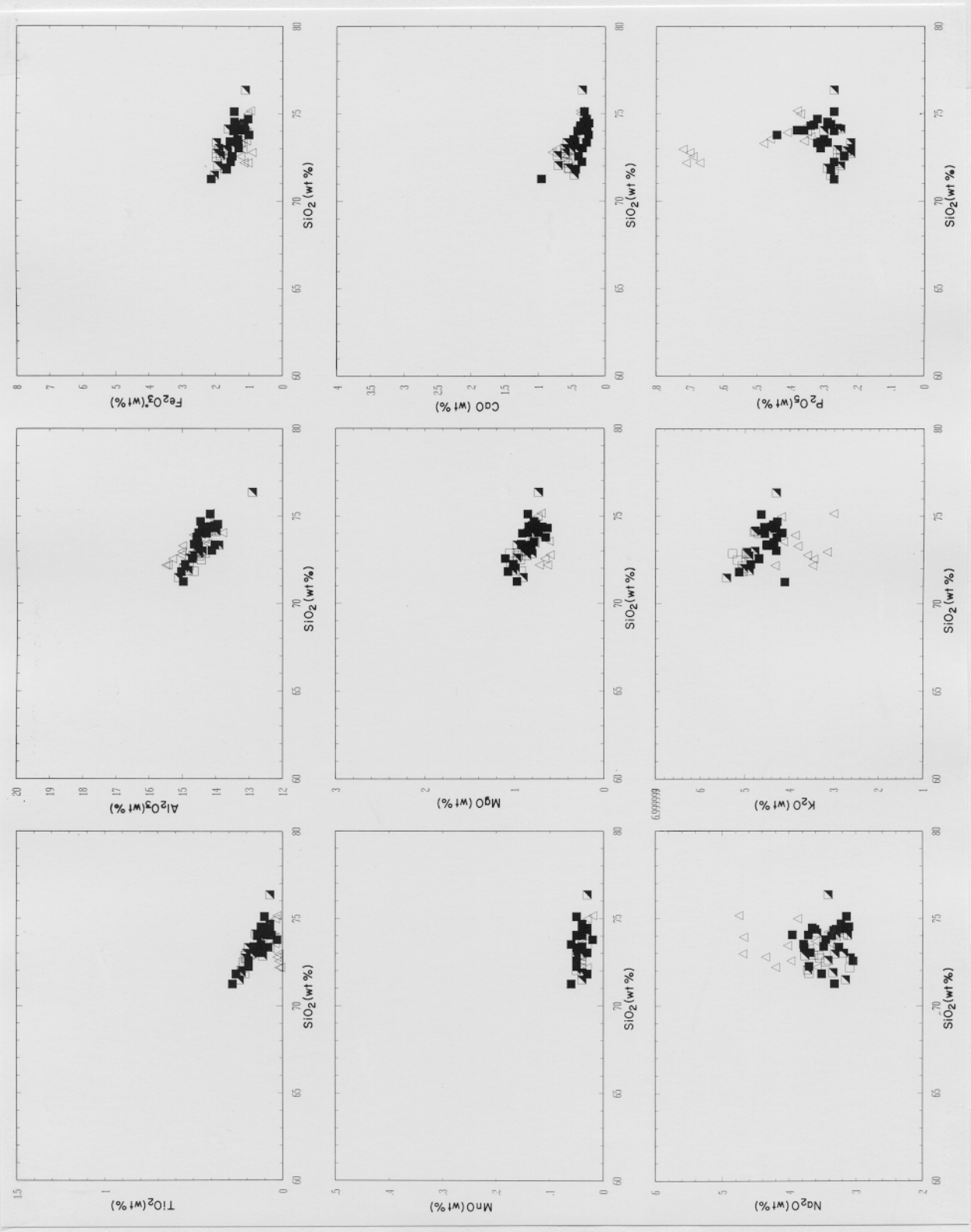

Figure 5.3e Harker variation diagrams for the East Dalhousie Stage II pluton.

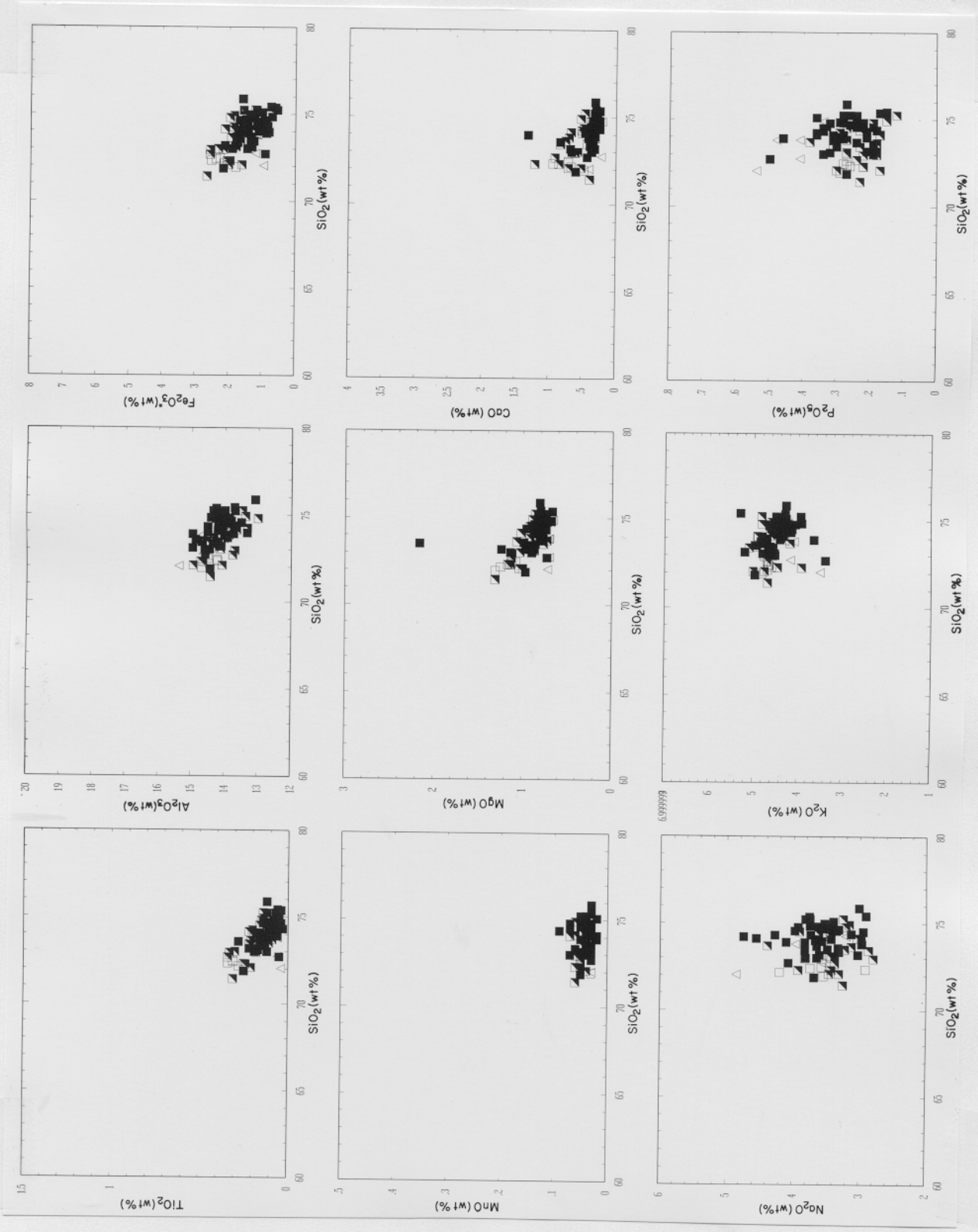

Figure 5.3f Harker variation diagrams for the New Ross Stage II pluton.

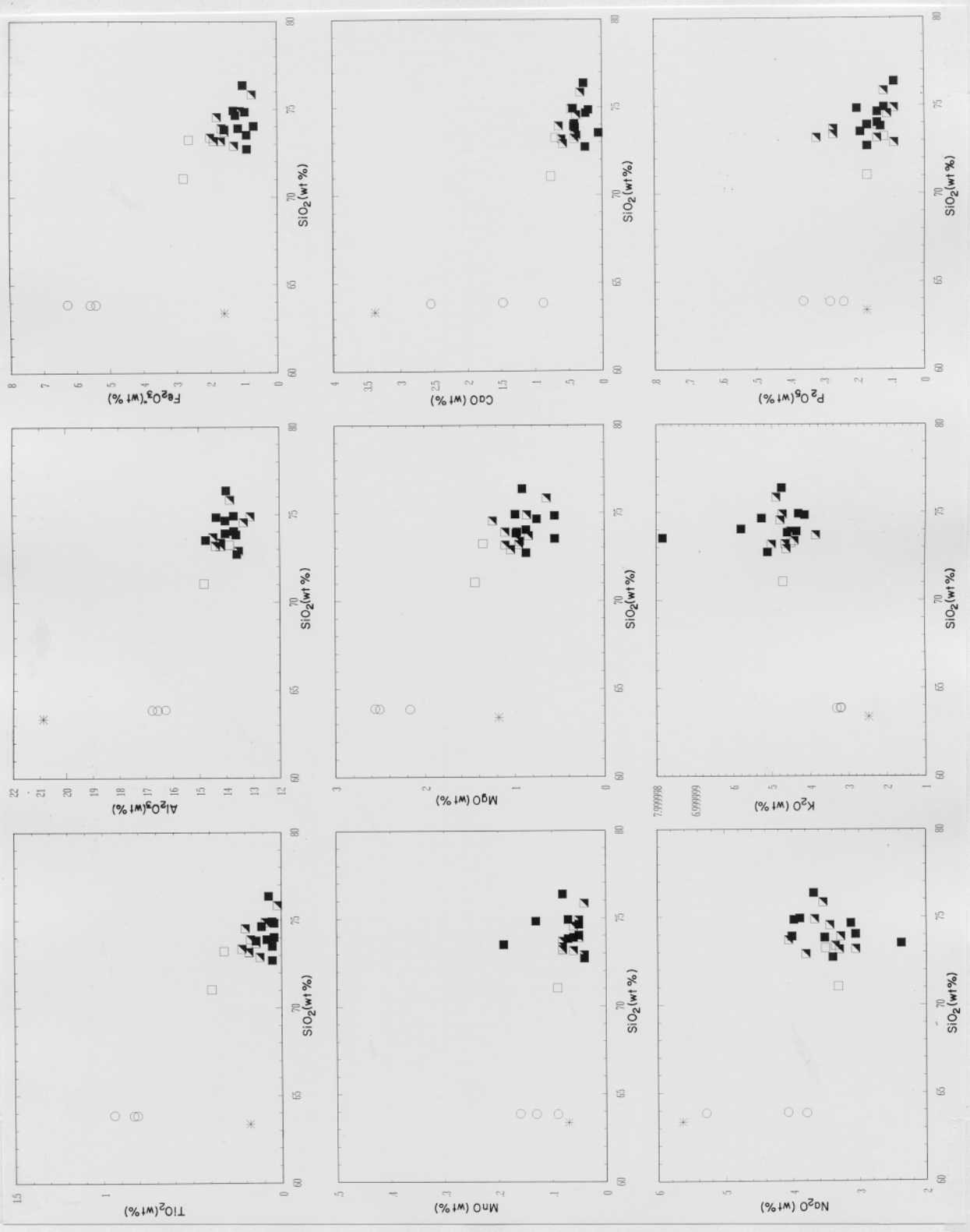

Figure 5.3g Harker variation diagrams for the Big Indian Lake Stage II pluton.

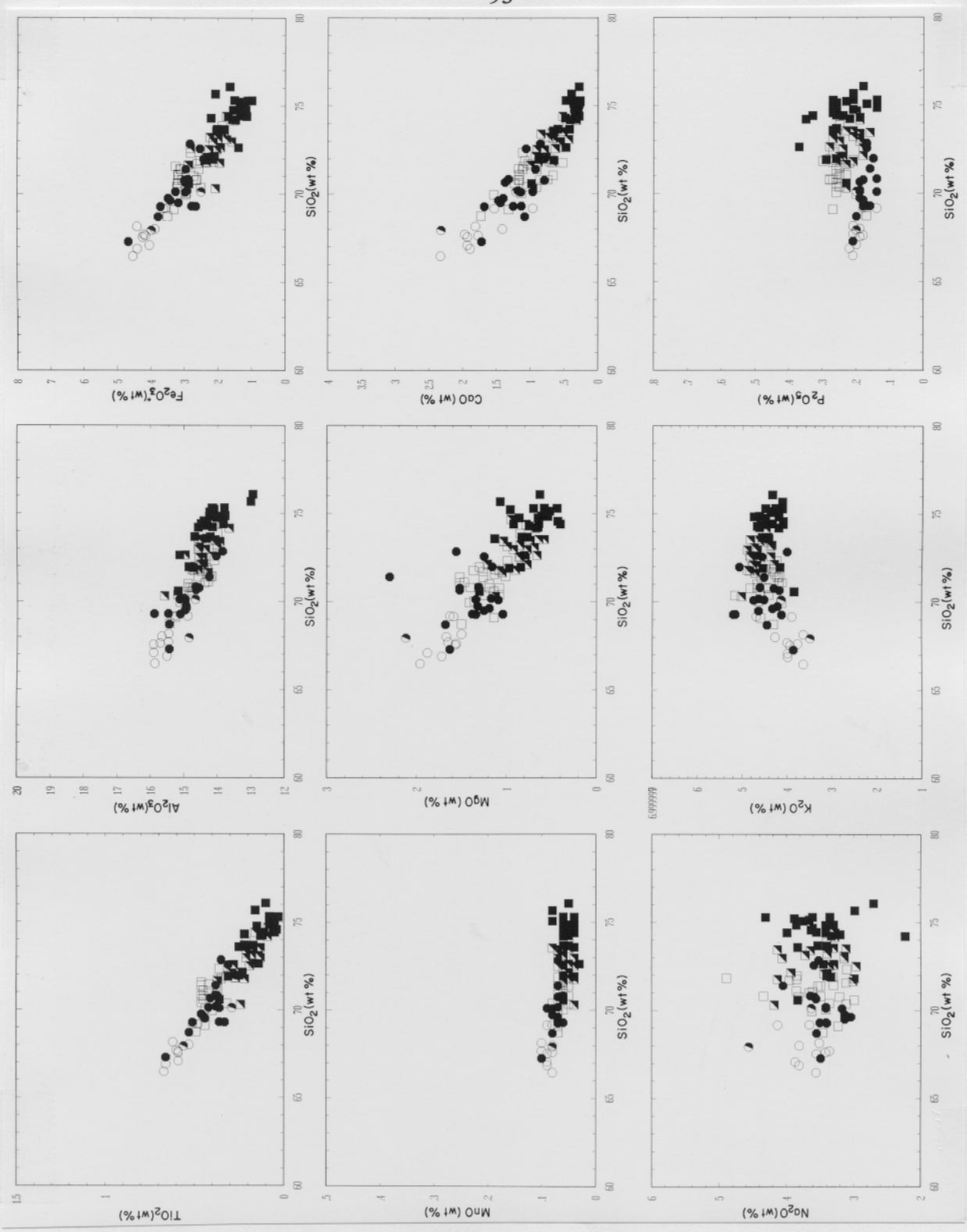

Figure 5.3h Harker variation diagrams for the Halifax Stage II pluton.

Table 5.1 Average major and trace element geochemistry and normative mineralogy of Stage I plutons

Pluton	Cloud Lake (CLP)			Five Island Lake (FIP)		Little Round Lake (LRP)	
Rock Type	BGD	BMG	FGLMG	BGD	APLI	BMG	FGLMG
% of Pluton	8.4	81.4	10.2	99.9	0.1	0	0
Samples	4	12	7	20	3	9	3
	Major Elements (wt %)						
SIO2	65.38	68.82	75.58	67.35	73.65	70.69	73.62
AL2O3	16.49	14.87	13.60	15.59	14.38	14.47	14.44
FE2O3	4.87	4.15	1.23	4.26	1.69	3.17	1.38
CAO	1.94	1.60	0.27	2.06	0.28	1.07	0.44
MGO	1.84	1.47	0.80	1.89	0.89	1.28	0.86
NA2O	3.36	3.35	3.77	3.53	3.08	3.12	3.64
K2O	3.63	4.08	4.33	3.56	4.68	4.27	4.47
TIO2	0.70	0.53	0.04	0.64	0.13	0.42	0.13
P2O5	0.21	0.19	0.14	0.21	0.18	0.21	0.30
MNO	0.11	0.09	0.06	0.08	0.02	0.08	0.05
H2O	0.95	0.34	0.42	0.69	1.33	0.65	0.64
	Normative Mineralogy						
Q	26.05	28.87	35.76	26.76	36.75	32.99	34.16
OR	21.84	24.33	25.65	21.21	27.91	25.57	26.64
AB	28.77	28.59	31.98	30.12	26.30	26.73	30.98
AN	8.31	6.78	0.39	8.95	0.35	3.96	0.26
C	4.11	2.50	2.57	2.70	4.17	3.32	3.55
EN	4.65	3.69	2.00	4.75	2.23	3.22	2.17
IL	0.24	0.19	0.08	0.17	0.05	0.17	0.12
HM	4.96	4.19	1.17	4.29	1.71	3.21	1.39
RU	0.58	0.43	0.00	0.56	0.11	0.33	0.06
AP	0.50	0.44	0.33	0.49	0.42	0.50	0.69
A/CNK	1.31	1.16	1.20	1.17	1.52	1.24	1.24
TTDI	76.66	81.78	93.38	78.09	90.96	85.29	91.77
Col. Ind.	9.83	8.07	3.33	9.21	4.00	6.61	3.67
	Trace Elements (ppm*)						
Ba	758	584	62	698	802	406	199
Rb	144	169	273	134	142	198	244
Sr	176	126	17	187	79	95	37
Zr	191	202	45	182	54	138	48
Nb	13	13	7	12	6	11	8
V	65	37	2	54	11	29	2
Y	34	42	24	29	21	33	19
Ga	21	18	17	22	16	17	16
Cu	19	4	7	6	3	7	0
Zn	78	61	33	86	24	59	26
Hf	6	7	2	6	2	4	1
Ta	1.1	1.2	1.7	1.0	0.7	1.4	1.8
Sc	12.4	9.8	3.0	10.4	3.6	7.7	2.7
La	36	35	4	36	10	24	7
Th	12.1	12.7	4.2	12.9	5.3	10.1	3.7
U	3.6	3.6	5.7	2.7	3.5	3.7	4.1
Li	59	60	47	49	14	75	89
F	531	672	205	601	230	624	403
As	5.9	6.5	13.2	1.3	94.6	5.6	6.1
Sn	1	6	3	7	10	8	12
W	0	1	5	1	1	2	3

Table 5.1 Average major and trace element geochemistry and normative mineralogy of

Pluton	Scrag Lake (SGP)			Salmontail Lake (STP)		
Rock Type	BGD	BMG	FGLMG	BGD	BMG	FGLMG
% of Pluton	21.2	78.4	0.4	8.3	91.2	0.5
Samples	23	21	22	3	30	5
SIO2	67.13	68.27	73.98	68.96	68.60	72.65
AL2O3	15.08	15.03	14.18	14.70	14.86	14.73
FE2O3	4.90	4.16	1.48	3.93	3.97	1.29
CAO	2.02	1.74	0.49	1.67	1.46	0.44
MGO	1.78	1.62	0.90	1.63	1.52	0.93
NA2O	3.18	3.30	3.51	3.30	3.44	3.61
K2O	3.73	4.02	4.73	3.78	4.02	4.72
TIO2	0.72	0.60	0.15	0.59	0.57	0.16
P2O5	0.21	0.21	0.20	0.19	0.22	0.28
MNO	0.09	0.08	0.05	0.08	0.09	0.04
H2O	0.51	0.57	0.52	0.69	0.61	0.60
Q	28.30	28.39	33.71	30.15	28.81	32.39
OR	22.30	23.98	28.09	22.64	24.06	28.22
AB	27.23	28.23	29.77	28.25	29.48	30.86
AN	8.74	7.36	1.20	7.13	5.85	0.48
C	2.67	2.60	2.86	2.62	2.77	3.55
EN	4.48	4.08	2.24	4.12	3.83	2.34
IL	0.20	0.18	0.10	0.17	0.18	0.08
HM	4.96	4.20	1.48	3.98	4.02	1.31
RU	0.62	0.51	0.10	0.51	0.47	0.12
AP	0.50	0.48	0.46	0.44	0.53	0.65
A/CNK	1.17	1.17	1.21	1.17	1.18	1.25
TTDI	77.82	80.60	91.56	81.04	82.35	91.46
Col. Ind.	9.64	8.45	3.83	8.26	8.03	3.73
Ba	684	613	242	546	525	402
Rb	152	156	220	148	165	205
Sr	157	136	56	132	123	52
Zr	220	188	67	174	181	71
Nb	13	12	10	12	12	9
V	62	51	5	47	42	5
Y	37	35	23	31	33	21
Ga	19	18	17	19	20	19
Cu	7	3	1	5	5	0
Zn	75	65	37	73	73	43
Hf	7	6	2	6	6	2
Ta	1.3	1.3	2.0	1.2	1.8	1.6
Sc	12.0	9.6	3.1	9.3	9.8	4.1
La	37	30	11	32	31	13
Th	13.3	11.6	5.9	11.6	11.7	7.3
U	3.0	3.4	5.2	2.6	3.6	5.5
Li	71	57	43	70	86	81
F	759	581	335	583	589	278
As	8.1	5.6	15.9	4.2	5.6	5.3
Sn	4	3	7	4	6	13
W	1	0	4	1	1	4

Table 5.2 Average major and trace element geochemistry and normative mineralogy of Stage II plutons

Pluton	Big Indian Lake (BIP)			Davis Lake (DLP)				
Rock Type	MBMG	CGLMG	FGLMG	BGD	MBMG	CGLMG	FGLMG	MLG
% of Pluton	1.8	81.4	16.8	1.3	0.6	93.9	3.6	0.5
Samples	2	9	9	2	5	29	2	5
SIO2	72.16	73.95	74.32	67.87	73.61	72.85	74.32	74.26
AL2O3	14.34	13.86	13.97	15.22	13.17	14.19	13.68	13.99
FE2O3	2.71	1.52	1.08	4.45	2.12	1.97	1.71	1.99
CAO	0.73	0.46	0.30	1.59	0.60	0.74	0.39	0.29
MGO	1.40	0.97	0.83	1.83	1.03	0.98	0.81	0.79
NA2O	3.41	3.49	3.44	3.32	3.54	3.57	3.38	3.13
K2O	4.61	4.60	5.13	3.91	4.47	4.52	4.06	4.10
TIO2	0.36	0.15	0.07	0.71	0.19	0.21	0.05	0.05
P2O5	0.15	0.17	0.15	0.23	0.12	0.21	0.17	0.24
MNO	0.09	0.06	0.08	0.10	0.06	0.05	0.08	0.08
H2O	0.75	0.68	0.49	0.75	0.78	0.57	1.20	1.08
Q	31.51	34.32	33.34	28.37	33.78	32.54	38.11	39.57
OR	27.27	27.44	30.53	23.29	26.72	26.89	24.35	24.49
AB	28.83	29.77	29.29	28.28	30.32	30.46	28.96	26.70
AN	2.65	1.18	0.64	6.45	2.21	2.31	0.83	0.13
C	2.78	2.72	2.53	3.22	1.72	2.60	3.48	4.41
EN	3.48	2.43	2.07	4.60	2.58	2.44	2.04	2.00
IL	0.18	0.12	0.11	0.21	0.13	0.10	0.09	0.10
HM	2.71	1.53	1.02	4.49	2.14	1.98	1.65	1.92
RU	0.26	0.08	0.01	0.60	0.12	0.16	0.00	0.00
AP	0.34	0.40	0.35	0.53	0.28	0.50	0.40	0.55
A/CNK	1.21	1.20	1.19	1.22	1.12	1.18	1.29	1.46
TTDI	87.60	91.52	93.16	79.93	90.81	89.90	91.40	90.76
Col. Ind.	6.37	4.09	3.30	9.29	4.85	4.53	3.89	4.14
Ba	403	173	102	579	151	244	24	25
Rb	190	198	185	167	495	334	744	946
Sr	96	38	21	143	33	54	6	14
Zr	125	58	39	188	95	104	34	33
Nb	10	8	5	11	14	12	21	24
V	22	9	3	55	13	9	0	0
Y	27	17	16	31	59	38	60	64
Ga	21	18	19	18	20	19	24	27
Cu	0	0	4	10	13	2	7	143
Zn	49	36	30	67	40	43	53	104
Hf	5	2	1	5	2	3	0	0
Ta	1.0	1.6	0.8	1.2	3.6	2.4	8.3	9.8
Sc	6.4	3.3	2.7	9.2	3.9	3.1	2.5	2.5
La	25	9	5	28	16	17	6	3
Th	12.0	4.9	2.8	12.0	18.0	12.8	12.5	11.8
U	3.9	4.1	4.0	3.4	20.2	10.1	18.3	27.5
Li	47	47	26	69	136	103	237	329
F	470	311	120	600	2686	1042	4034	3900
As	0.8	2.2	1.2	1.5	1.9	2.2	0.0	2.3
Sn	9	9	9	6	19	13	27	204
W	2	1	1	0	26	3	63	19

Table 5.2 Average major and trace element geochemistry and normative mineralogy of Stage II plutons

Pluton	East Dalhousie (EDP)				Halifax (HP)			
Rock Type	MBMG	CGLMG	FGLMG	MLG	BGD	MP	BMG	MBMG
% of Pluton	0	0	0	0	4.1	0.1	12.6	33.3
Samples	6	13	21	16	10	2	18	25
SIO2	72.50	73.20	73.65	73.58	67.79	69.04	70.24	71.07
AL2O3	14.53	14.38	14.41	14.62	15.55	14.75	14.88	14.63
FE2O3	1.77	1.71	1.37	1.19	4.10	3.24	3.13	2.83
CAO	0.56	0.49	0.38	0.45	1.75	1.77	1.20	1.03
MGO	0.98	0.88	0.84	0.74	1.67	2.86	1.39	1.23
NA2O	3.49	3.36	3.45	3.87	3.67	4.10	3.44	3.56
K2O	5.07	4.82	4.45	3.96	3.98	3.82	4.51	4.47
TIO2	0.21	0.17	0.12	0.05	0.58	0.43	0.41	0.39
P2O5	0.25	0.25	0.31	0.47	0.19	0.20	0.18	0.25
MNO	0.04	0.04	0.04	0.04	0.09	0.08	0.07	0.06
H2O	0.55	0.52	0.64	0.80	0.67	0.60	0.62	0.65
Q	31.01	33.75	35.50	35.09	25.65	23.11	28.95	30.06
OR	30.16	28.73	26.54	23.65	23.70	22.51	26.82	26.58
AB	29.73	28.59	29.48	33.01	31.22	34.57	29.29	30.23
AN	1.13	0.86	0.23	0.00	7.48	7.19	4.83	3.46
C	2.90	3.34	3.87	3.99	2.49	1.23	2.59	2.69
EN	2.45	2.20	2.11	1.86	4.19	7.02	3.48	3.08
IL	0.10	0.09	0.09	0.06	0.19	0.16	0.15	0.13
HM	1.78	1.72	1.38	1.18	4.13	3.24	3.15	2.85
RU	0.16	0.12	0.08	0.02	0.49	0.34	0.33	0.32
AP	0.59	0.59	0.72	1.11	0.45	0.46	0.41	0.59
A/CNK	1.19	1.24	1.29	1.28	1.15	1.06	1.17	1.17
TTDI	90.90	91.07	91.53	91.76	80.57	80.18	85.06	86.87
Col. Ind.	4.33	4.01	3.58	3.12	8.51	10.60	6.79	6.06
Ba	307	170	129	33	588	354	469	360
Rb	297	322	377	557	164	201	198	242
Sr	54	36	27	13	171	120	122	92
Zr	99	75	55	32	177	119	140	132
Nb	14	12	13	22	12	11	11	14
V	6	6	3	2	44	35	29	26
Y	23	23	21	26	32	22	30	24
Ga	19	20	21	27	22	20	21	22
Cu	1	0	1	1	1	2	2	3
Zn	51	54	48	50	71	59	66	65
Hf	3	3	1	1	6	3	4	4
Ta	2.1	2.1	3.2	4.0	1.1	1.4	1.2	1.7
Sc	3.0	2.5	2.8	2.6	9.4	7.2	6.7	5.8
La	20	13	8	4	34	22	27	24
Th	13.8	9.8	5.3	3.4	12.3	10.0	11.6	11.2
U	4.7	4.7	4.9	3.1	3.0	4.0	3.6	4.3
Li	96	113	153	149	76	95	88	93
F	1045	1223	1134	1953	646	650	638	710
As	4.1	2.6	6.1	2.7	4.6	4.3	2.3	2.9
Sn	11	13	22	25	5	14	7	9
W	3	2	5	6	1	1	1	1

Table 5.2 Average major and trace element geochemistry and normative mineralogy of Stage II plutons

Pluton	Halifax (HP) Cont.		Kejimkujik (KP)	Morse Road (MRP)		New Ross (NRP)	
Rock Type	CGLMG	FGLMG	MBMG	CGLMG	FGLMG	MBMG	CGLMG
% of Pluton	37.6	12.3	100	0	0	11.6	59.3
Samples	24	27	3	3	2	5	27
SIO2	72.85	74.29	69.90	71.95	72.94	72.27	73.57
AL2O3	14.35	14.20	15.15	15.08	14.40	14.43	14.05
FE2O3	2.04	1.59	3.48	2.00	1.90	2.22	1.84
CAO	0.68	0.42	0.94	0.66	0.70	0.70	0.56
MGO	0.88	0.73	1.49	1.09	1.23	1.18	0.95
NA2O	3.46	3.47	3.09	3.15	3.25	3.60	3.39
K2O	4.64	4.38	4.29	5.22	4.97	4.69	4.64
TIO2	0.20	0.13	0.46	0.28	0.25	0.30	0.19
P2O5	0.22	0.24	0.24	0.21	0.17	0.27	0.24
MNO	0.06	0.05	0.09	0.04	0.05	0.05	0.05
H2O	0.57	0.72	0.83	0.57	0.55	0.55	0.50
Q	33.00	36.15	32.22	31.31	32.25	30.97	34.29
OR	27.62	26.03	25.58	30.95	29.42	27.81	27.57
AB	29.49	29.50	26.37	26.71	27.51	30.56	28.85
AN	1.92	0.59	3.16	1.92	2.37	1.69	1.27
C	2.95	3.55	4.32	3.57	2.82	2.81	3.00
EN	2.21	1.83	3.74	2.71	3.06	2.95	2.37
IL	0.12	0.11	0.20	0.10	0.10	0.10	0.10
HM	2.05	1.59	3.51	2.01	1.90	2.22	1.85
RU	0.14	0.07	0.36	0.23	0.20	0.25	0.14
AP	0.51	0.57	0.55	0.49	0.40	0.64	0.56
A/CNK	1.20	1.27	1.33	1.26	1.20	1.18	1.21
TTDI	90.10	91.68	84.17	88.98	89.18	89.34	90.72
Col. Ind.	4.38	3.53	7.44	4.82	5.05	5.27	4.31
Ba	199	101	556	391	376	273	205
Rb	278	329	196	268	217	312	311
Sr	55	28	108	79	80	58	48
Zr	84	59	148	117	105	126	83
Nb	11	11	10	14	11	14	12
V	11	7	41	11	15	16	9
Y	23	19	27	23	24	24	25
Ga	22	21	17	19	16	20	19
Cu	0	1	0	0	0	0	1
Zn	51	47	58	55	43	62	51
Hf	3	2	4	4	4	3	3
Ta	1.9	2.4	1.7	1.6	1.3	1.9	2.1
Sc	4.0	3.2	6.3	3.4	3.4	3.9	3.4
La	15	8	27	27	24	22	15
Th	8.2	5.1	11.0	16.3	13.0	17.9	9.8
U	5.8	8.8	4.8	5.1	5.3	3.8	5.5
Li	95	108	76	78	79	105	107
F	763	759	534	562	479	1495	1135
As	3.7	5.5	1.6	5.7	4.2	71.9	2.4
Sn	12	20	3	7	4	11	14
W	2	6	1	0	0	7	3

Table 5.2 Cont.

Pluton	NRP Cont.		West Dalhousie (WD	
Rock Type	FGLMG	MLG	CGLMG	FGLMG
% of Pluton	27.6	1.5	99.5	0.5
Samples	41	7	11	3
SIO2	74.19	73.77	72.44	73.66
AL2O3	14.16	14.50	14.49	14.45
FE2O3	1.30	1.28	2.00	1.35
CAO	0.39	0.29	0.65	0.42
MGO	0.86	0.72	1.07	0.94
NA2O	3.61	3.77	3.15	3.17
K2O	4.45	4.15	4.97	4.60
TIO2	0.11	0.07	0.27	0.16
P2O5	0.27	0.40	0.21	0.26
MNO	0.04	0.03	0.04	0.03
H2O	0.57	0.63	0.62	0.67
Q	34.83	35.17	32.90	36.36
OR	26.49	24.73	29.61	27.45
AB	30.75	32.13	26.84	27.11
AN	0.42	0.00	1.90	0.42
C	3.25	3.84	3.26	4.13
EN	2.17	1.80	2.67	2.36
IL	0.09	0.07	0.10	0.07
HM	1.31	1.29	2.01	1.36
RU	0.07	0.04	0.23	0.13
AP	0.63	0.94	0.48	0.62
A/CNK	1.24	1.30	1.23	1.32
TTDI	92.07	92.03	89.36	90.91
Col. Ind.	3.56	3.16	4.78	3.79
Ba	116	39	364	158
Rb	356	785	251	292
Sr	25	18	67	35
Zr	53	44	107	56
Nb	12	27	12	14
V	2	2	12	5
Y	23	33	21	20
Ga	21	28	18	19
Cu	3	0	0	0
Zn	43	71	52	46
Hf	2	2	3	1
Ta	2.4	6.3	1.7	3.1
Sc	3.1	2.1	3.2	2.1
La	8	4	27	13
Th	5.7	6.2	17.0	8.8
U	9.1	4.5	5.0	8.7
Li	93	410	80	98
F	1161	3884	638	554
As	6.8	1.5	5.7	8.2
Sn	18	34	6	11
W	6	10	1	3

The sequence biotite granodiorite (± mafic porphyry) → biotite monzogranite → muscovite-biotite monzogranite → coarse-grained leucomonzogranite → fine-grained leucomonzogranite → muscovite leucogranite in both Stage I and II plutons is marked by systematic decreases in TiO_2, Fe_2O_3, MgO and CaO with increasing SiO_2. Al_2O_3 also decreases with increasing SiO_2 in most plutons with the exception of the Little Round Lake and Salmontail Lake Stage I plutons where Al_2O_3 levels are roughly constant throughout. MnO values generally show limited decrease with increasing SiO_2. In contrast the large variation in MnO values in the Cloud Lake pluton, particularly in biotite-rich mafic porphyry and dyke rocks, and in the fine-grained leucomonzogranite of the Big Indian Lake pluton, are for samples that contain Mn-rich garnet. In general Na_2O and K_2O do not show well-defined compositional trends for the main rock types in the Stage I and II plutons. However, it should be noted that some rocks do show enrichment or depletion in these elements that presumably reflect variable degrees of alteration. For example, The enrichment in Na_2O and concomitant depletion in K_2O in the muscovite leucogranite of the East Dalhousie pluton may reflect albitization with the "stripping" of K_2O by fluids. P_2O_5 is mainly constant with increasing SiO_2 for the majority of rocks in both Stage I and II plutons but shows strong enrichment in leucomonzogranite and leucogranite in several Stage II plutons.

The sequence biotite granodiorite → muscovite leucogranite is also marked by decreases in normative anorthite, enstatite, ilmenite, hematite, rutile and colour index and several "compatible" trace elements (i.e. Ba, Sr, Zr, V, Hf, Sc and La) and increases in normative quartz, A/CNK and Thornton-Tuttle differentiation index and several "incompatible" trace elements (i.e. Rb, Ta, U, Li, F, Sn and W). Elements considered to be "compatible" are preferentially

partitioned into mineral phases during crystal fractionation and therefore are depleted in later-staged rocks. Conversely "incompatible" elements are preferentially partitioned into the melt and/or fluid phase during crystallization of a magma and will therefore become enriched in the more evolved, late-staged rocks. Some "incompatible" elements are incorporated into mineral phases, such as Rb in the phyllosilicate minerals, and some "compatible" elements may become enriched in some late-staged rocks, for example high P_2O_5 in some leucogranite bodies. It should also be noted that some elements may change from compatible to incompatible behaviour during the crystallization history of a given granite body as a result of varying physico-chemical conditions. Thus, these terms are simply meant as guides to the overall behaviour of individual elements.

It is apparent from the major and trace element data and normative mineralogy (Tables 5.1, 5.2, Appendix A; Figures 5.2 and 5.3) that the amount of overall chemical variability differs between the various Stage I and Stage II plutons. For example the Stage II Halifax pluton, containing granodiorite, monzogranite and leucomonzogranite rock units, markedly contrasts with the Morse Road and Kejimkujik plutons that are dominated by compositionally restricted monzogranite and leucomonzogranite rocks. Similarly the Stage I Scrag Lake pluton, which displays a wide compositional range, is in marked contrast to the more compositionally restricted Little Round Lake pluton.

The chemical data also reveal compositional differences between the rock types in various plutons. For example, coarse-grained leucomonzogranite in the Davis Lake pluton has a much larger compositional range (e.g. SiO_2 ca. 67-75 wt %), than the same rock type in the Halifax and West Dalhousie plutons (e.g. SiO_2 ca. 70.5-74 wt %), New Ross pluton (e.g. SiO_2 ca. 71.5-

75.5 wt %), and the Big Indian Lake pluton (e.g. SiO_2 ca. 73-75.5 wt %).

Several major element "discriminating" diagrams have been developed specifically for intrusive rocks. Data for average rock types from Stage I and II plutons have been plotted on a multi-cationic plot (Debon and LeFort, 1983) and is shown in Figure 5.4. This plot classifies samples based on the relative proportions of the quartzo-feldspathic elements Si, K, Na and Ca. Only the most "primitive" samples of mafic porphyry and granodiorite from Stage I and II plutons, plot near the granodiorite field (#3) with most data being split between the "adamellite" field (i.e. monzogranite -#2) and "granite" (i.e. syenogranite - #1) fields. There is no clear relationship between the measured quartz-alkali feldspar-plagioclase determinations from Chapter 4, and the positions of the major rock types in Figure 5.4. For example the least evolved "granodiorite" from Stage I and II plutons and the most evolved leucogranite from the Stage II plutons plot in the "adamellite" field.

Debon and LeFort (1983) also developed a multi-cationic diagram that specifically classifies granitoid rocks into peraluminous versus metaluminous groups and estimates the proportions of biotite, muscovite and hornblende. Plots of the average rock-type compositions for Stage I and II plutons are given in Figures 5.5a and b. Unlike the results for Figure 5.4, there is a remarkable agreement between the measured and predicted modal mineralogy. Firstly, all rocks correctly plot in the peraluminous field. Secondly, only the mafic porphyry and some biotite granodiorite units plot in the "biotite only" field (#III), biotite granodiorite, biotite monzogranite, muscovite-biotite monzogranite and leucomonzogranite all plot in the "biotite > muscovite" field (#II). Only fine-grained leucomonzogranite and leucogranite plot in the "muscovite" field (#I). None of the samples plot in the "hornblende + biotite" field (#IV) which is in accord with the

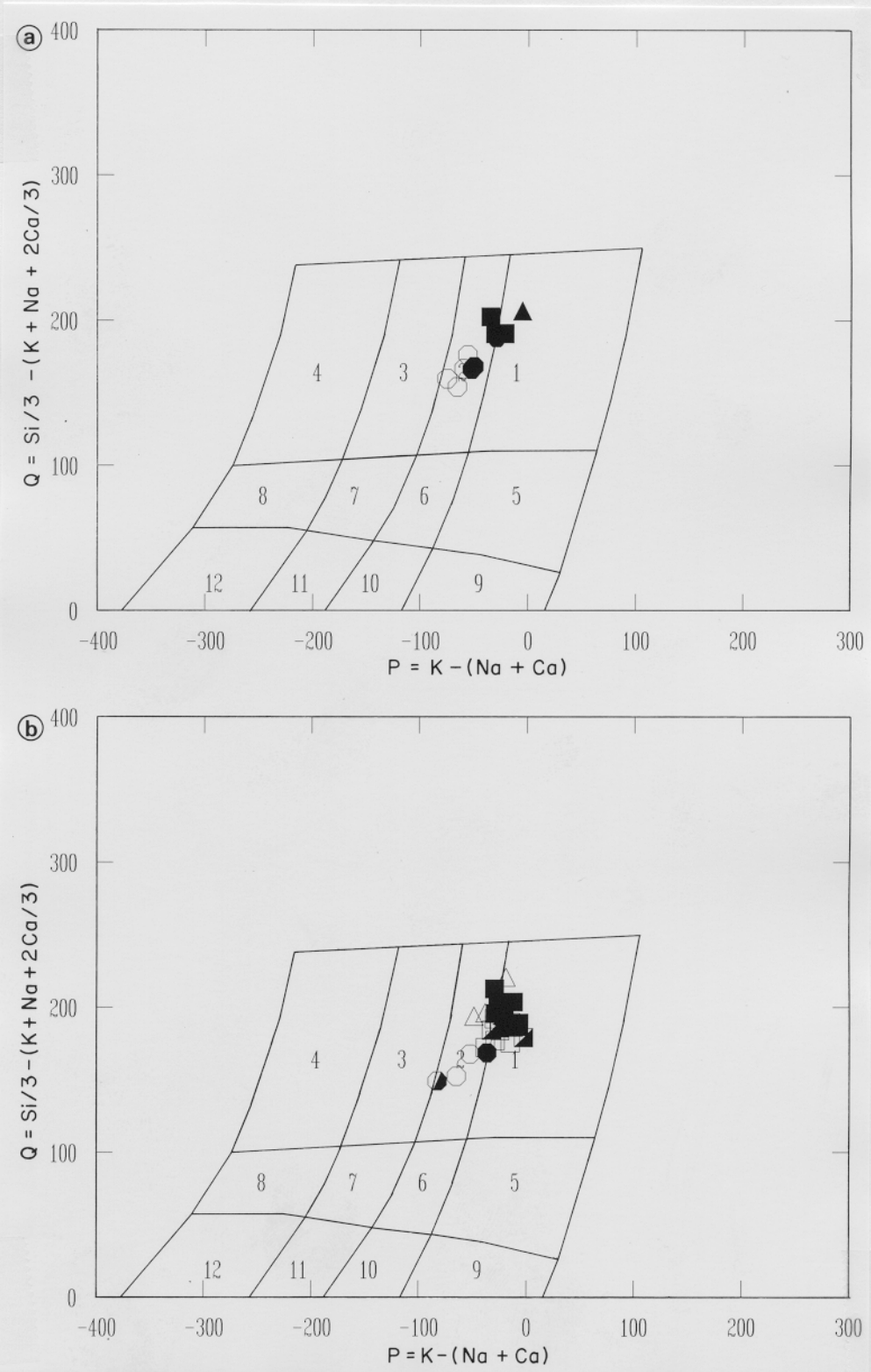

Figure 5.4 Multi-cationic plot (after Debon and LeFort, 1983) of average rock type for: a) Stage I plutons; b) Stage I plutons. Fields include #3 - granodiorite; #2 - monzogranite; #1 - syenogranite. See text for discussion.

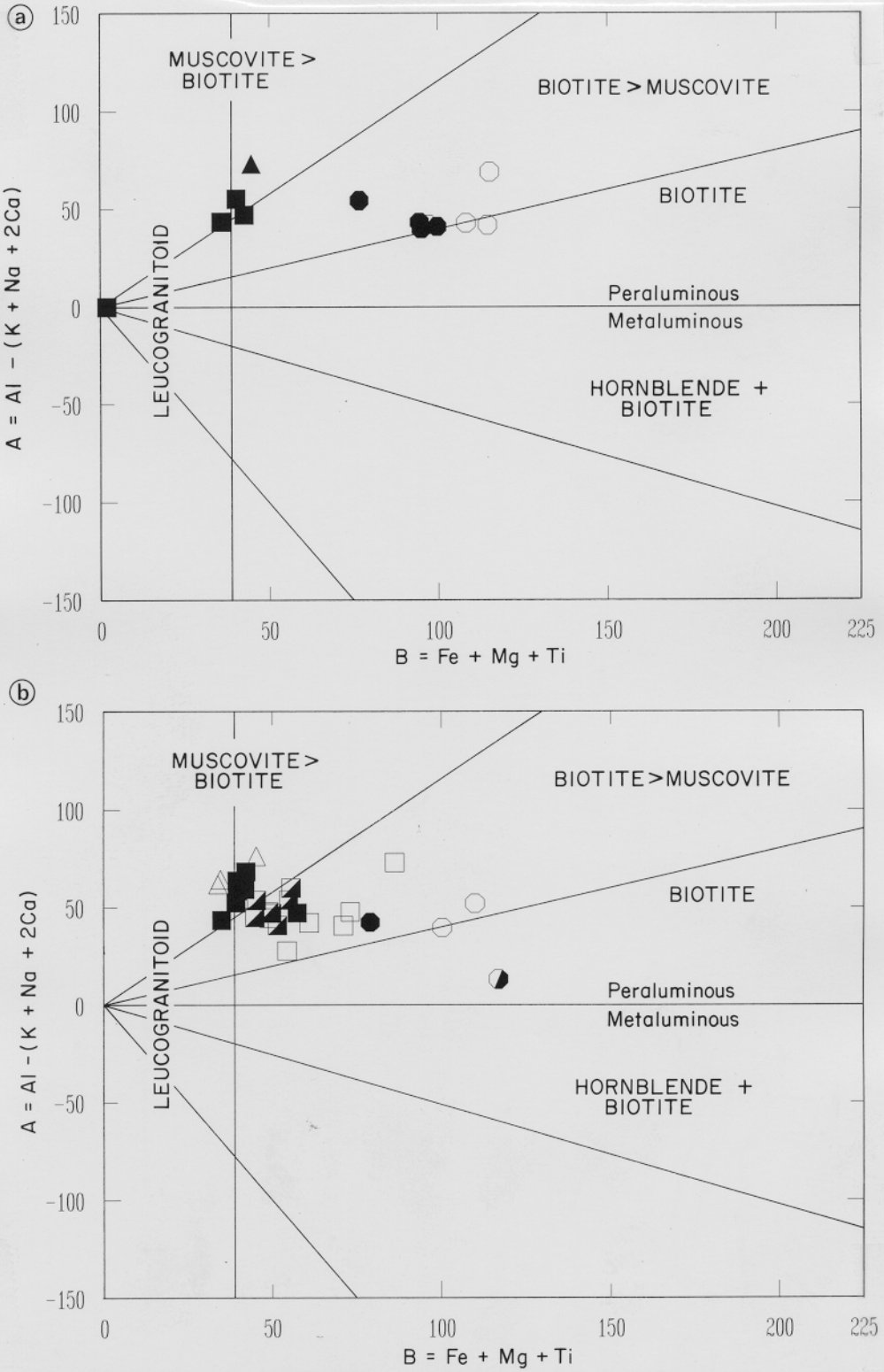

Figure 5.5 Multi-cationic plot (after Debon and LeFort, 1983) of average rock types for a) Stage I plutons; b) Stage II plutons. Note that all rocks plot in the peraluminous fields. See text for discussion.

observed petrographic data. Finally, only two leucogranite and two fine-grained leucomonzogranite bodies plot in the "leucogranitoid" field which supports the field observations from this study.

Middlemost (1985) presented a classification scheme for igneous rocks that was based on the proportions of SiO_2 versus $Na_2O + K_2O$. Virtually all data from both Stage I and II plutons (Figs. 5.6a,b) plot in the "granite" (i.e. monzogranite and syenogranite fields; #6) with two granodiorite units correctly plotting in the granodiorite field (#11).

Ternary plots of normative quartz, alkali feldspar and plagioclase for Stage I and II plutons are given in Figures 5.7a and b (fields after LeMaitre, 1989). The granodiorite and mafic porphyry units from all plutons plot correctly in the granodiorite field. All other rock units plot in the monzogranite field with nearly complete overlap for all rock types. The chief reason for the lack of separation between these latter rock types is that normative albite is combined with normative anorthite (i.e. P) whereas the A apex is only made up of normative orthoclase. Therefore the shift toward syenogranite and even alkali feldspar granite that was shown in Figures 5.4 and 5.6 is absent in the LeMaitre (1989) plot. Streckeisen (1976) concluded that albitic plagioclase with $An_{<5}$ should be combined with K-feldspar. Unfortunately normative programs do not provide an estimate of the relative proportions of albite with $An_{<5}$ and $An_{>5}$ which prohibits the generation of a normative equivalent to the Streckeisen (1976) diagram. Plots of the proportions of anorthite versus albite + orthoclase for the Scrag Lake Stage I and New Ross Stage II plutons have been prepared to further illustrate this problem and are displayed in Figures 5.8a and b. Lines of equal proportions (e.g.1:2 An:Ab + Or) have also been included.

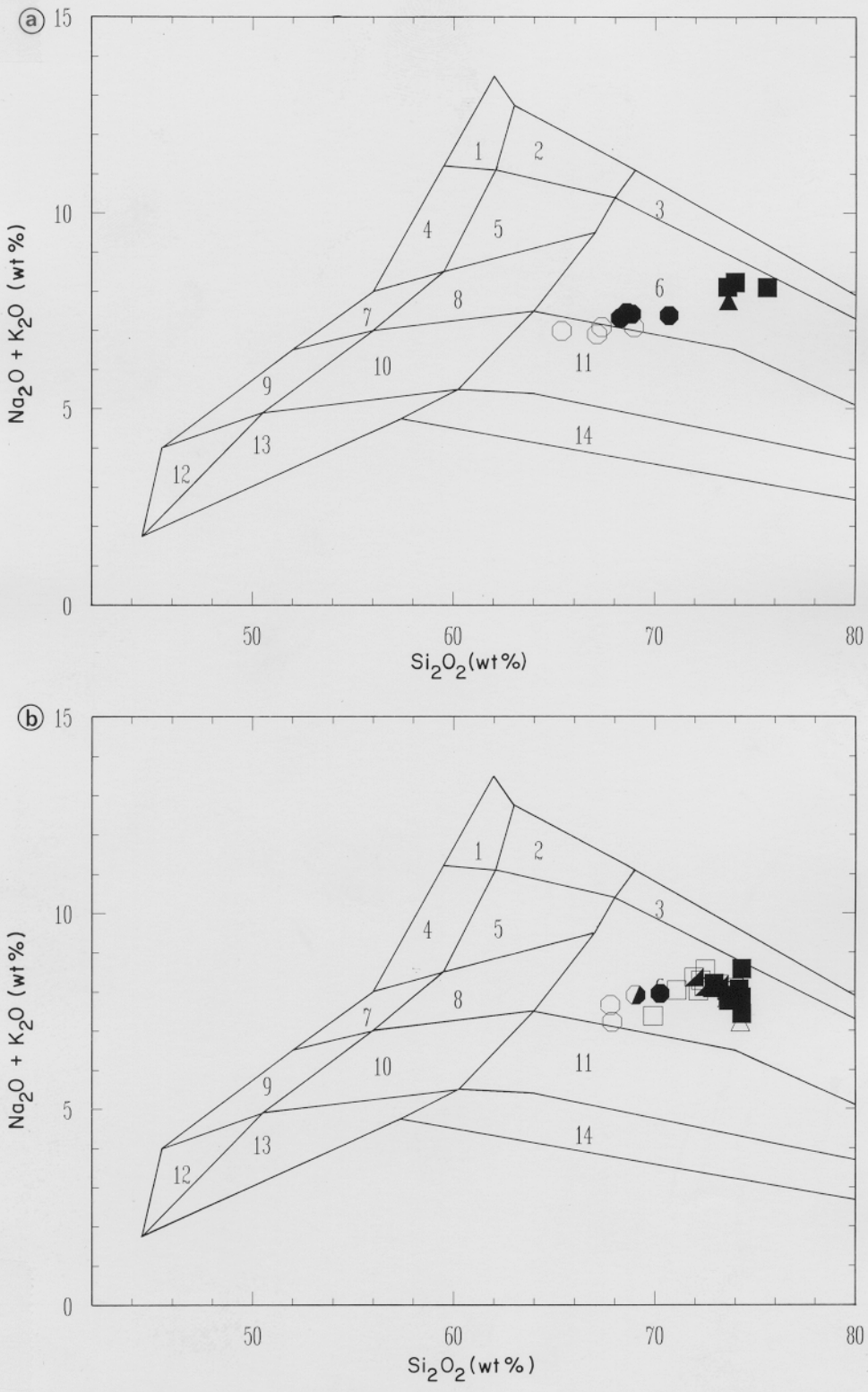

Figure 5.6 Average rock data for Stage I and II plutons plotted on classification scheme of Middlemost (1985). a) Stage I plutons; b) Stage II plutons. See text for discussion.

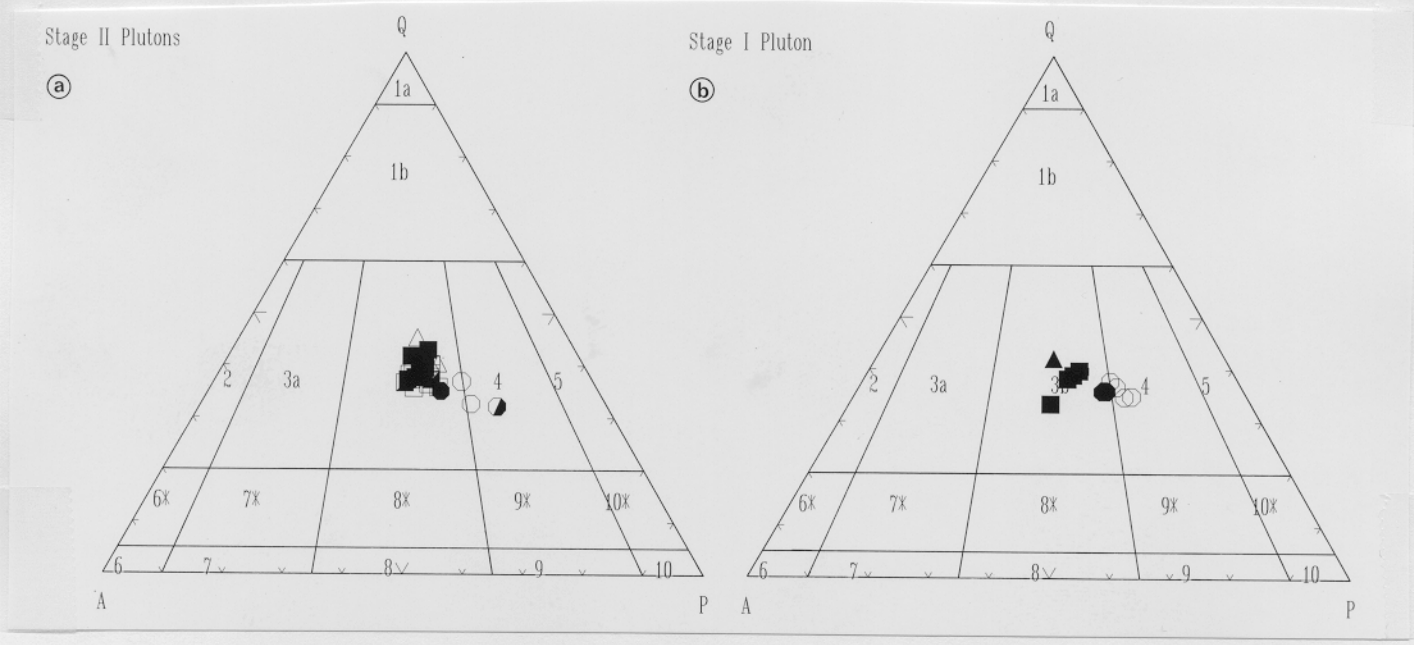

Figure 5.7 Ternary plots of average CIPW normative data for Stage I and II plutons (fields after LeMaitre, 1989). a) Stage I plutons; b) Stage II plutons. See text for discussion.

When all albite is assigned to alkali feldspar, which clearly is not accurate in light of the petrographic information presented in Chapter 4, then granodiorite and biotite monzogranite from the Scrag Lake Stage I pluton plot in the syenogranite field Fig 5.8a). Fine grained leucomonzogranite from this pluton and all samples from the New Ross pluton plot in the alkali feldspar field. Clearly the amount of shift toward alkali feldspar granite compositions is beyond what is predicted from the observed mineralogy. Therefore accurate designation of rock types for the batholith on the basis of normative mineralogy is not possible using available classification schemes. Proper classification will only be possible if the relative proportion of albite with $An_{<5}$ and $An_{>5}$ can be determined.

5.2.2 Chemical Zoning in Stage I and II Plutons

Most Stage I and II plutons are compositionally zoned with individual plutons displaying normal, reverse or normal & reverse zoning (MacDonald and Horne, 1988; Horne et al., 1989;

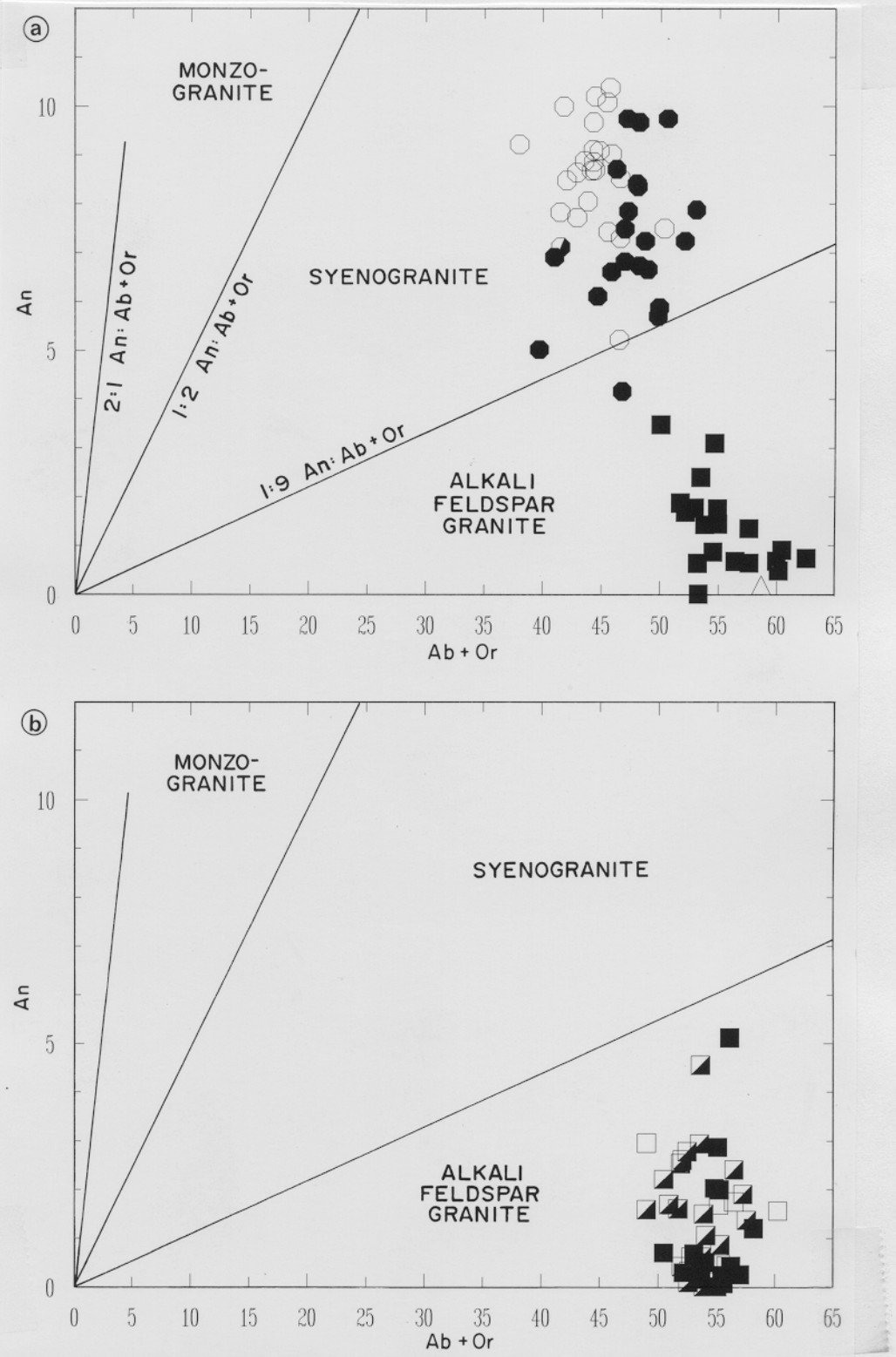

Figure 5.8 Binary plots of normative anorthite (An) versus albite (Ab) + orthoclase (Or) for total data sets from: a) Scrag Lake Stage I pluton; and b) New Ross Stage II pluton. See text for discussion.

MacDonald et al., 1992). Normal zoning consists of plutons with least "evolved" compositions at or near the pluton margins and most "evolved" rock compositions in pluton cores. Reverse zoning, as the name implies, consists of more evolved margins and less evolved cores. The following section outlines a few examples of compositional zoning patterns from both Stage I and II plutons.

The Salmontail Lake Pluton displays the most consistent and symmetrical compositional zoning of the five Stage I plutons, as shown in Figures 5.9a to c. Concentrations of the "compatible" elements Sr and Zr are clearly highest along the pluton margins (>140 ppm Sr and >210 ppm Zr) and lowest (<100 ppm Sr and <150 ppm Zr) in two regions of the pluton core. Conversely the highest concentrations of the "incompatible" element Rb are generally lowest along the pluton margins (<140-160 ppm) with highest values predominating the core of the pluton (>180 ppm). These patterns, and indeed the trends for most major and trace elements, are consistent with normal zoning as defined above. It should be noted that the most evolved rocks of the Salmontail Lake pluton, the Gold River fine-grained leucomonzogranite bodies, are situated in the most evolved portion of the pluton. O'Reilly (1992) has noted spatial association, and has proposed genetic relationships, between the New Ross Manganese Mines and the Gold River leucomonzogranite bodies. The positioning of mineral deposit and leucomonzogranite in the most evolved part of the large biotite monzogranite unit in the core of the Salmontail Lake pluton may be merely coincidental, but more likely indicates some degree of genetic association.

The Davis Lake Stage II Pluton has normal compositional zoning as shown in Figure 5.10a to f). The highest values of K/Rb (>200), which as stated above is a dependable indicator

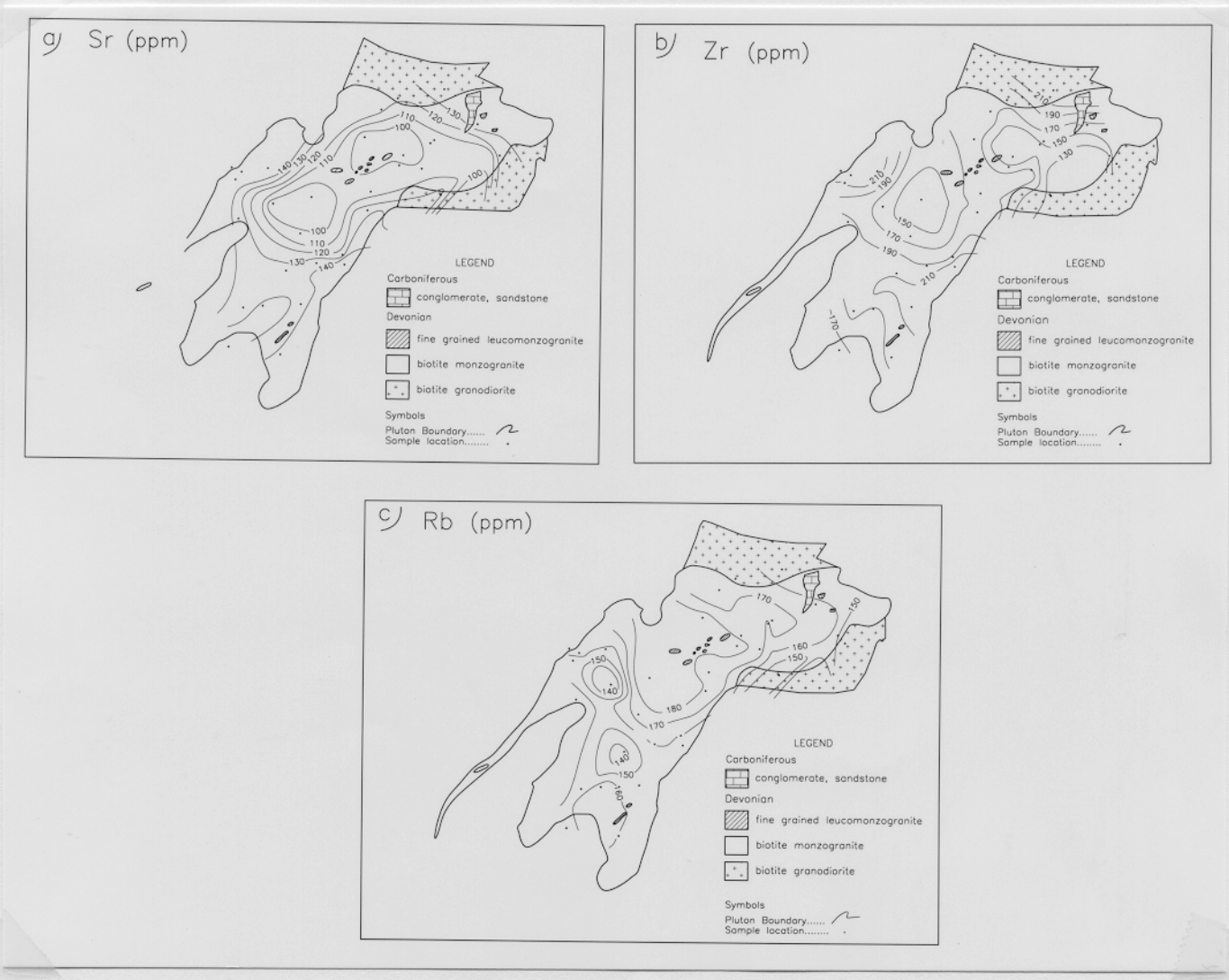

Figure 5.9 Lithogeochemical contour plots for biotite monzogranite and biotite granodiorite from the Stage I Salmontail Lake Pluton. See text for discussion.

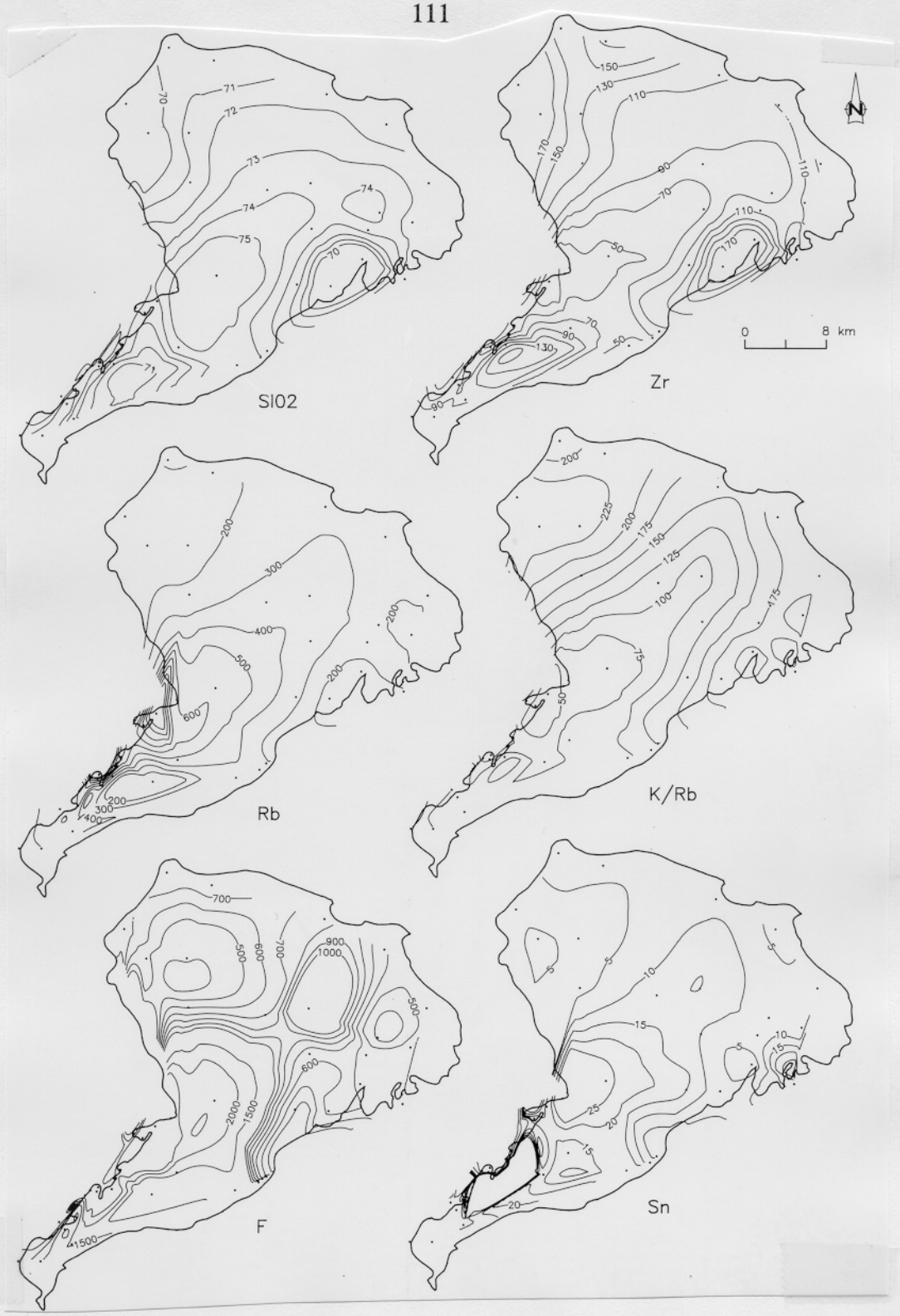

Figure 5.10 Lithogeochemical contour plots for coarse-grained leucominzogranite and biotite monzogranite from the Stage II Davis Lake Pluton. See text for discussion.

of the degree of differentiation, are for samples located along the northern and southeastern margins of the pluton. There is a progressive decrease in K/Rb toward the southwestern extension of the pluton where the lowest values (50-100) predominate. This transition from northern margin to the East Kemptville area is also marked by a decrease in most "compatible" elements (e.g. Zr) and increase in most "incompatible" elements (e.g. Rb, F, Sn). It is worthy of note that the East Kemptville leucogranite, and Sn deposit, resides in the most evolved part of the pluton, much like the Gold River leucomonzogranite bodies in the Salmontail pluton. In fact, Chatterjee and MacDonald (1991) successfully established a genetic link between the coarse-grained leucomonzogranite, the muscovite-topaz leucogranite and greisens from the East Kemptville Sn deposit using rare earth element geochemistry. Therefore it appears that there may be a causal relationship between the processes that generated regional-scale compositional zoning in plutons and the formation of mineral deposits. Kontak (1994) has also proposed that the East Kemptville deposit was formed by prolonged fractionation of the Davis Lake Pluton.

The Halifax Pluton is the best example of normal and reverse zoning in a Stage II pluton. Contour plots of Zr and Rb and a 3-dimensional perspective plot of Rb/Zr for data from the Halifax Pluton are presented in Figure 5.11a to c respectively. The western part of the pluton displays very systematic normal zoning with high Zr (>200 ppm) and low Rb (<180 ppm) and Rb/Zr in the granodiorite and biotite monzogranite along the margin to low Zr (<80 ppm) and high Rb (>320 ppm) and Rb/Zr in the core regions. In contrast the eastern portion of the pluton displays normal compositional zoning near the margin, as developed to the west, but has a reversely zoned core. The reader is referred to MacDonald and Horne (1988) for a detailed discussion of possible mechanisms for development of the observed zoning features. In simplistic

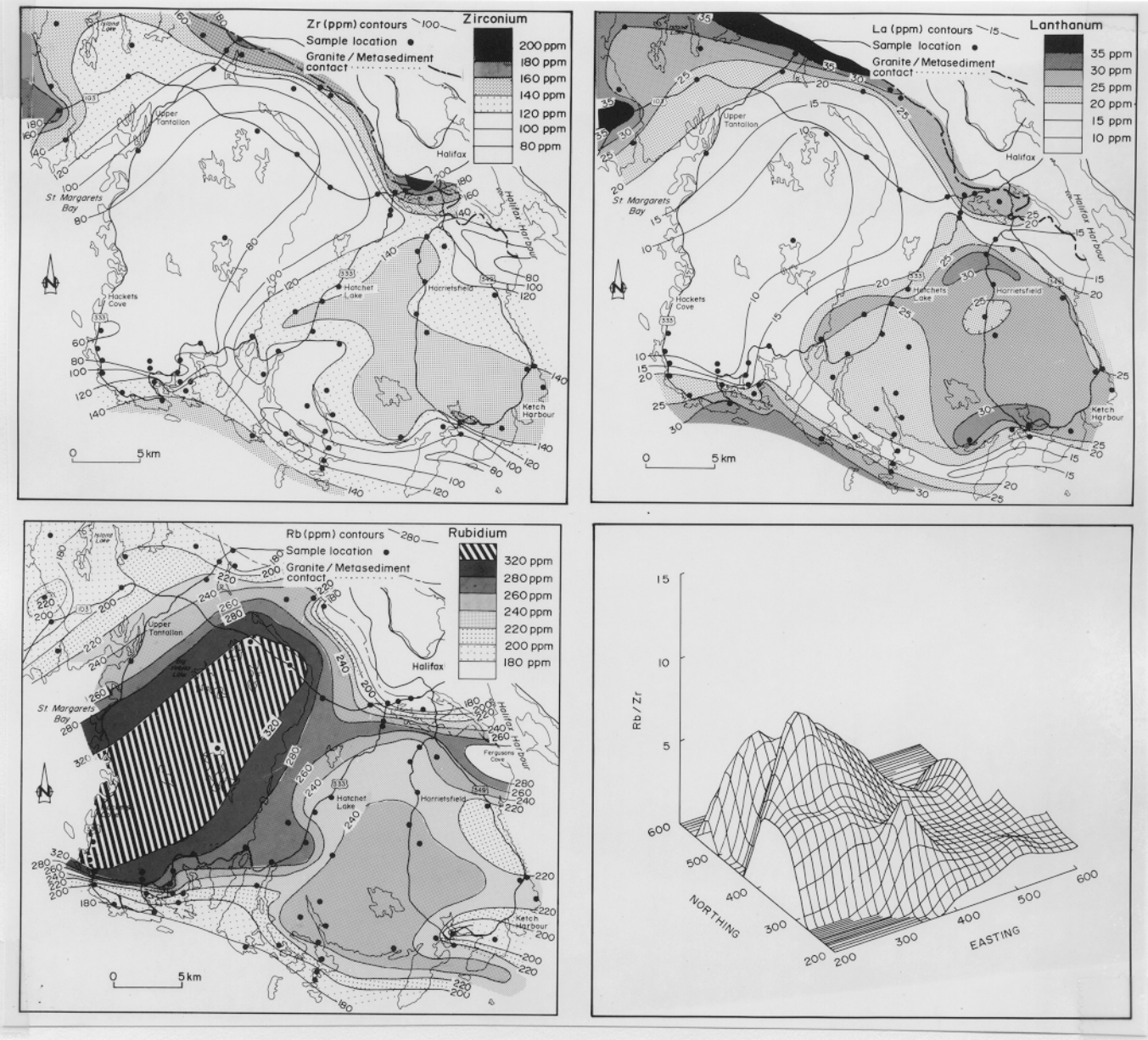

Figure 5.11 Lithogeochemical contour plots and 3-Dimensional plot for biotite granodiorite, biotite monzogranite, muscovite-biotite monzogranite and coarse-grained leucominzogranite from the Stage II Halifax Pluton. See text for discussion.

terms, MacDonald and Horne (1988) concluded that the zoning was formed by a combination of sidewall fractional crystallization along "cool" metasedimentary chamber walls, coupled with the development of vertical stratification, and subsequent upwelling of magma within a central

magma chamber.

The presence of both normal and reverse zoning in the sundry plutons of the batholith requires that zoning is not simply formed by static *in situ* fractional crystallization from margin to core of plutons because this process should only result in normally zoning. A comprehensive discussion of the various processes responsible for formation of zoning is beyond the scope of this report.

5.2.3 Comparison of Various Stage I & II Plutons

The above data indicate that the five Stage I and eight Stage II plutons have broadly similar chemical characteristics. Despite these overall similarities it is possible to distinguish among individual Stage I and II plutons. For example, binary element plots of TiO_2 versus Zr and Ta versus F have been prepared for the Big Indian Lake and New Ross Stage II plutons (fig. 5.12a to d). TiO_2 and Zr are very strongly correlated in both plutons ($R=+0.98$ and $+0.97$, respectively). However, the overall concentrations of these elements, and the slopes of regression lines, vary between the two plutons (Fig. 5.12a,b). The respective concentrations and distribution of Ta and F also vary between the two plutons, as displayed in Figures 5.12c and d.

Much of the chemical differences between individual plutons are more subtle that those shown in Figure 5.12 and are very difficult to recognize using conventional bivariate or ternary elemental plots. Smith (1979) used multivariate statistical techniques to separate several Stage II plutons in the SMB. An evaluation of his data in light of recent mapping indicates that his sample sets consisted of a combination of Stage I and II plutons and therefore are not considered to present an accurate depiction of the chemistry of Stage II plutons.

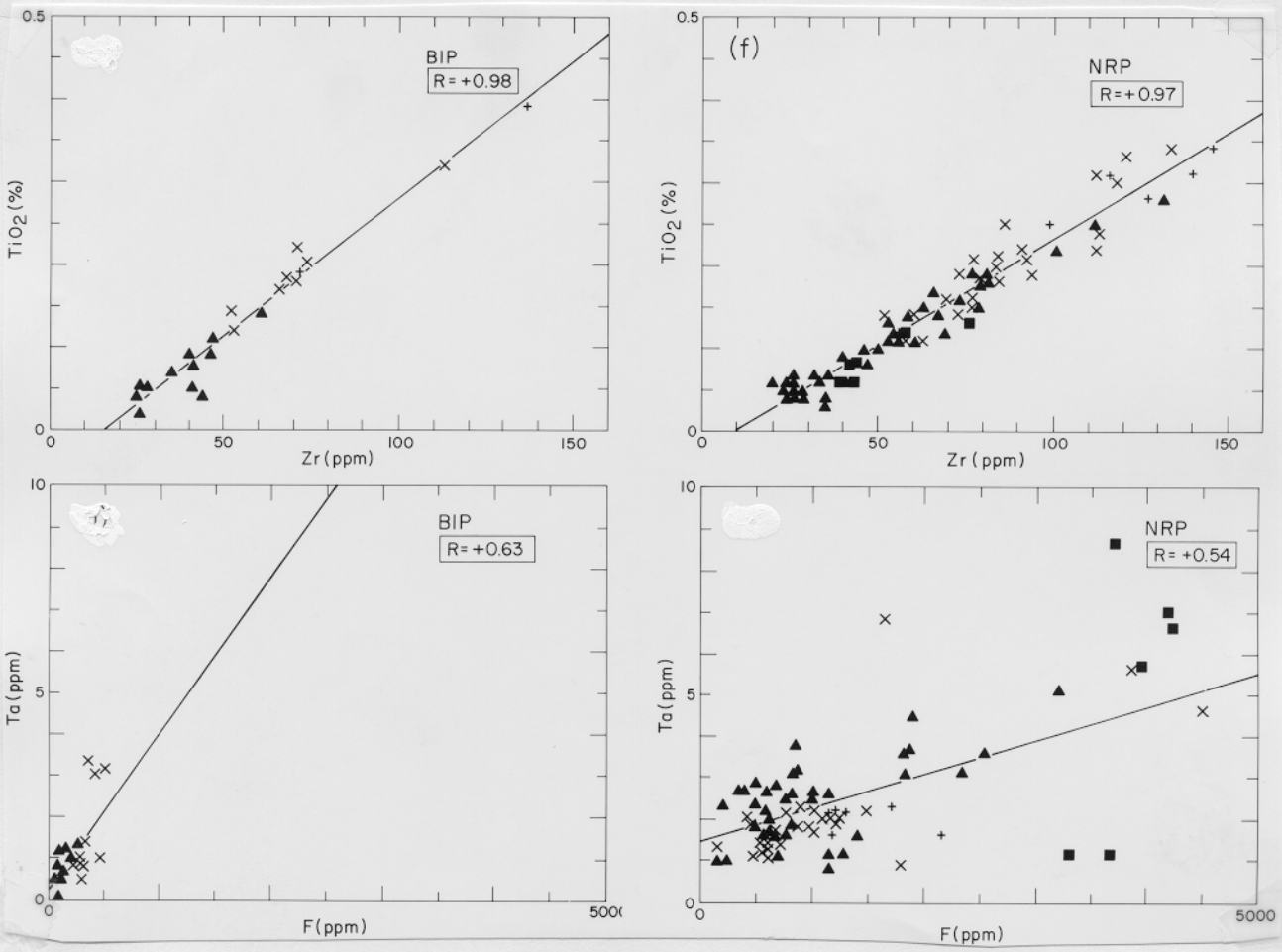

Figure 5.12 Bivariate plots for the Big Indian Lake and New Ross Stage II plutons. See text for discussion.

Horne et al. (1989) recognized chemical differences among biotite granodiorite and biotite monzogranite bodies from several Stage I plutons using multi-variate discriminant function analysis. They used a suite of high field strength elements (TiO_2, Fe_2O_3, Zr, Hf and Y) and concluded that the compositional differences between the various plutons resulted from variations in the mineral chemistry of biotite and the varying proportions of the associated accessory minerals zircon and xenotime entrained within this biotite. It should be noted that while there was little overlap in discriminant function scores between the various Stage 1 plutons, the within-group

variance generally exceeded the between-group separation. Therefore, one of the main mathematical criteria for reliable discrimination was not satisfied. It is possible that chemical distinctions between the various plutons might be successfully recognized (i.e. satisfying all mathematical criteria) by using step-wise multiple discrimination as noted by Chatterjee and Strong (1984) in their study of metasomatized uraniferous rocks in the batholith.

MacDonald et al. (1992) separated coarse-grained leucomonzogranite samples from six of the Stage II plutons including Davis Lake, West Dalhousie, East Dalhousie, New Ross, Big Indian Lake and Halifax. They then applied the same multi-variate techniques and suite of elements as Horne et al. (1989) to determine if the Stage II plutons could be discriminated. Their results indicate that samples from four of the plutons (Davis Lake, West Dalhousie, Big Indian Lake, and Halifax) could be correctly assigned to their respective bodies with a 70-85 % success rate, with the same mathematical restrictions as noted above. Conversely, the success rate for samples from the New Ross and East Dalhousie plutons was less convincing at only a 25 % success rate. Samples from these plutons were commonly misclassified as belonging to the other pluton or, to a lesser extent, to one of the above plutons suggesting a genetic relationship between these two plutons.

It is possible to distinguish between Stage II plutons using rare earth element (REE) data for a specific rock type. Sample suites from muscovite-biotite monzogranite units in the Halifax, New Ross, West Dalhousie, Kejimkujik and Davis Lake plutons were analyzed for REE (unpublished data A.K. Chatterjee, 1993). It should be stressed that most samples from muscovite-biotite monzogranite, with the exception of some rocks from the DLP, have $K/Rb > 150$, and thus are interpreted as "pristine magmatic" rocks. Plots of the REE analyses for the five units are plotted in Figure 5.13. Samples from each pluton show very cohesive geochemical behaviour with

consistent light (LREE) and heavy (HREE) fractionation patterns and Eu/Eu*. In contrast, the REE patterns differ significantly among the various plutons. For example the rocks from the Halifax, Kejimkujik and New Ross plutons have fractionated patterns with similar ratios of LREE to HREE and similar Eu `anomalies'. The unit from the Davis Lake pluton has a very "flat" pattern with very low LREE/HREE ratios and large Eu `anomaly'. The MBMG unit from the West Dalhousie pluton has a very fractionated HREE pattern and a large Eu `anomaly'.

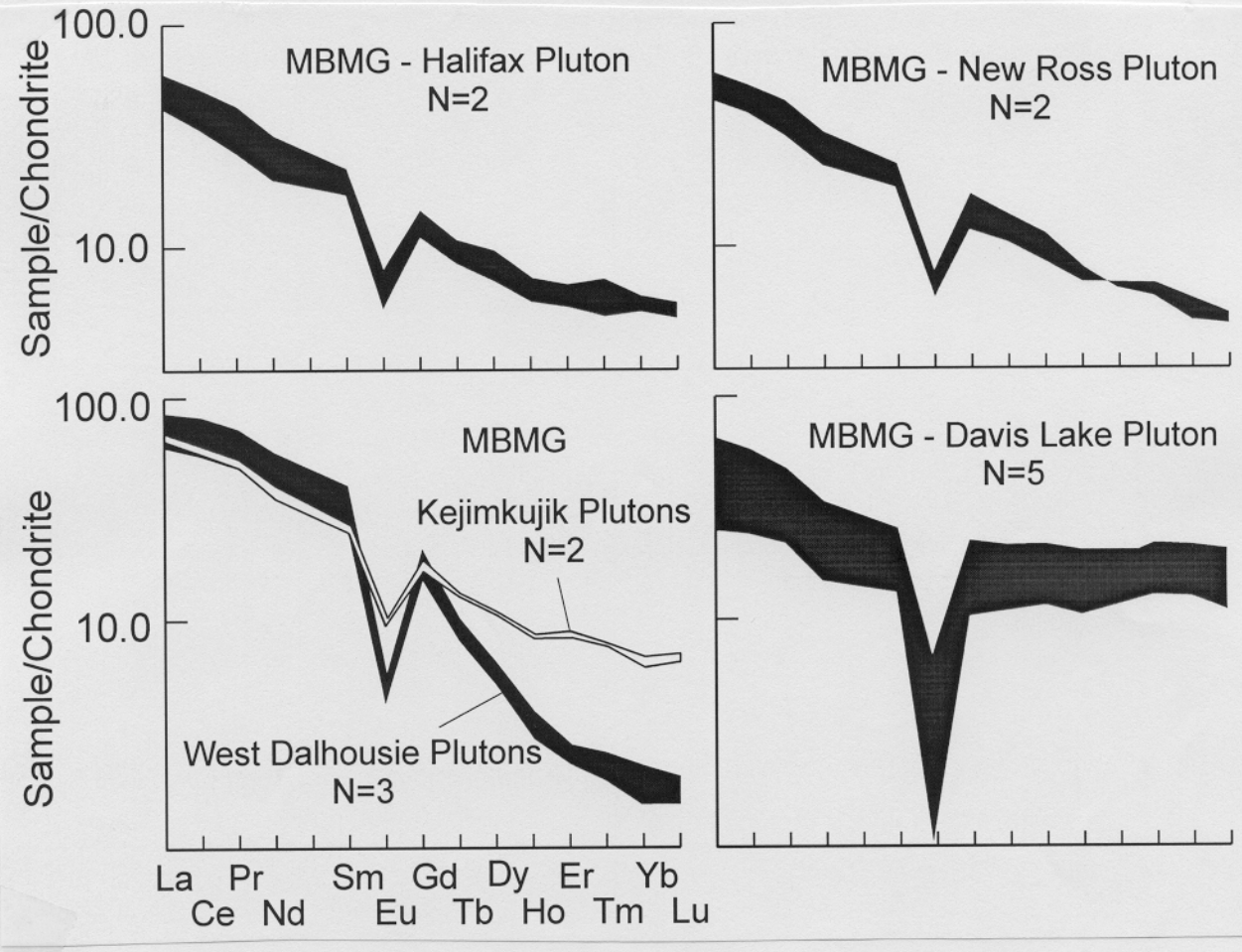

Figure 5.13 Rare Earth Element (REE) plots for muscovite-biotite monzogranite from the Halifax, New Ross, Kejimkujik, West Dalhousie and Davis Lake Stage II plutons. See text for discussion.

The high values for K/Rb in these rocks preclude an explanation of the observed REE spectra by fluid-related alteration and/or metasomatism. Therefore, the differences in major, trace

and REE data among the various Stage II plutons must result from one or more of the following factors: 1) differing physico-chemical conditions during crystallization of sundry plutons, possibly resulting in differing accessory mineral assemblages (monazite, zircon, xenotime, apatite); 2) differing compositions of the "parental" magmas for the various plutons, presumably reflecting differences in the protolith composition and/or varying degrees of partial melting in the protolith. It is not possible to reconcile the viability of these two processes, given the available data.

5.2.3 Geochemistry of Leucogranite Rocks

Leucogranite rocks are the most `evolved' rocks in the batholith, are frequently spatially associated with, and commonly interpreted to be the progenitors of, polymetallic mineral deposits. Consequently, the chemical make-up of these rocks deserves special attention.

Chemical analyses of muscovite leucogranite rocks (MLG) from the batholith are presented in Appendix A. Previous workers have noted significant differences in the compositions of leucogranitic rocks of the batholith. Kontak et al. (1988) defined two types of leucogranites, corresponding to leucogranite and leucomonzogranite of this study, which were characterized using trace element and $^{18}\delta O$ geochemistry. Clarke et al. (1993) also described two leucogranite types using major, trace and rare earth element and $^{18}\delta O$ geochemistry. Their "independent" leucogranite bodies correspond to leucogranite of this study whereas their "associated" leucogranites occur as portions of fine-grained leucomonzogranite which have undergone fluid-related alteration. Chatterjee and MacDonald (1993) established a four-fold subdivision of leucogranite using the trace element data in Appendix A and REE geochemistry (unpubl. data A.K. Chatterjee). They noted two main groups: Group A "non-specialized" leucogranites with high K/Rb, Eu/Eu^*, Nb/Ta, and high levels of "compatible" elements (e.g. Ba), and low Rb/Sr

and low concentrations of "incompatible" elements (e.g. F, Li, Rb, Ta, Nb and Sn); and Group B "specialized" leucogranites with high Rb/Sr and high concentrations of "incompatible" elements and low K/Rb, Eu/Eu^*, Nb/Ta, and low levels of "compatible" elements.

Group A non-specialized leucogranites can further be subdivided into A_1, including the Walsh Brook leucogranites (Corey, 1987). These MLG have high P_2O_5 (0.30%) and low MnO (0.03%) compared with average biotite granodiorite compositions (0.21% P_2O_5; 0.08% MnO). These rocks also have "fractionated" REE patterns (Figure 5.14a) with large Gd/Lu_N (3.64) and La/Lu_N (5.78). A second subgroup A_2, which includes the Big Indian Lake leucogranites (Corey, 1987), have low P_2O_5 (0.15%) and high MnO (0.12%) compared to granodiorite, and have "V" shaped REE spectra (Fig. 5.14b) with very low values of Gd/Lu_N (0.36) and La/Lu_N (0.96).

Group B specialized leucogranites can further be subdivided into B^1 which include the East Kemptville leucogranites and outcrop at, and adjacent to, the East Kemptville Sn mine (Ham and MacDonald, 1994), the Murphy Lake leucogranite (MacDonald and Ham, 1992), and the Keddy-Reeves and Lake Lewis leucogranites from the New Ross area (Horne, 1993; Ham, 1990). Rocks of this subgroup have high P_2O_5 (0.44%) and low MnO (0.04%), compared to granodiorite, and display "fractionated" REE patterns (Figure 5.14c) with moderate Gd/Lu_N (3.01) and La/Lu_N (5.40). A second subgroup B_2, which includes the Davis Lake and Dog Lake leucogranites (Ham and MacDonald, 1994), have low P_2O_5 (0.16%) and high MnO (0.08%)

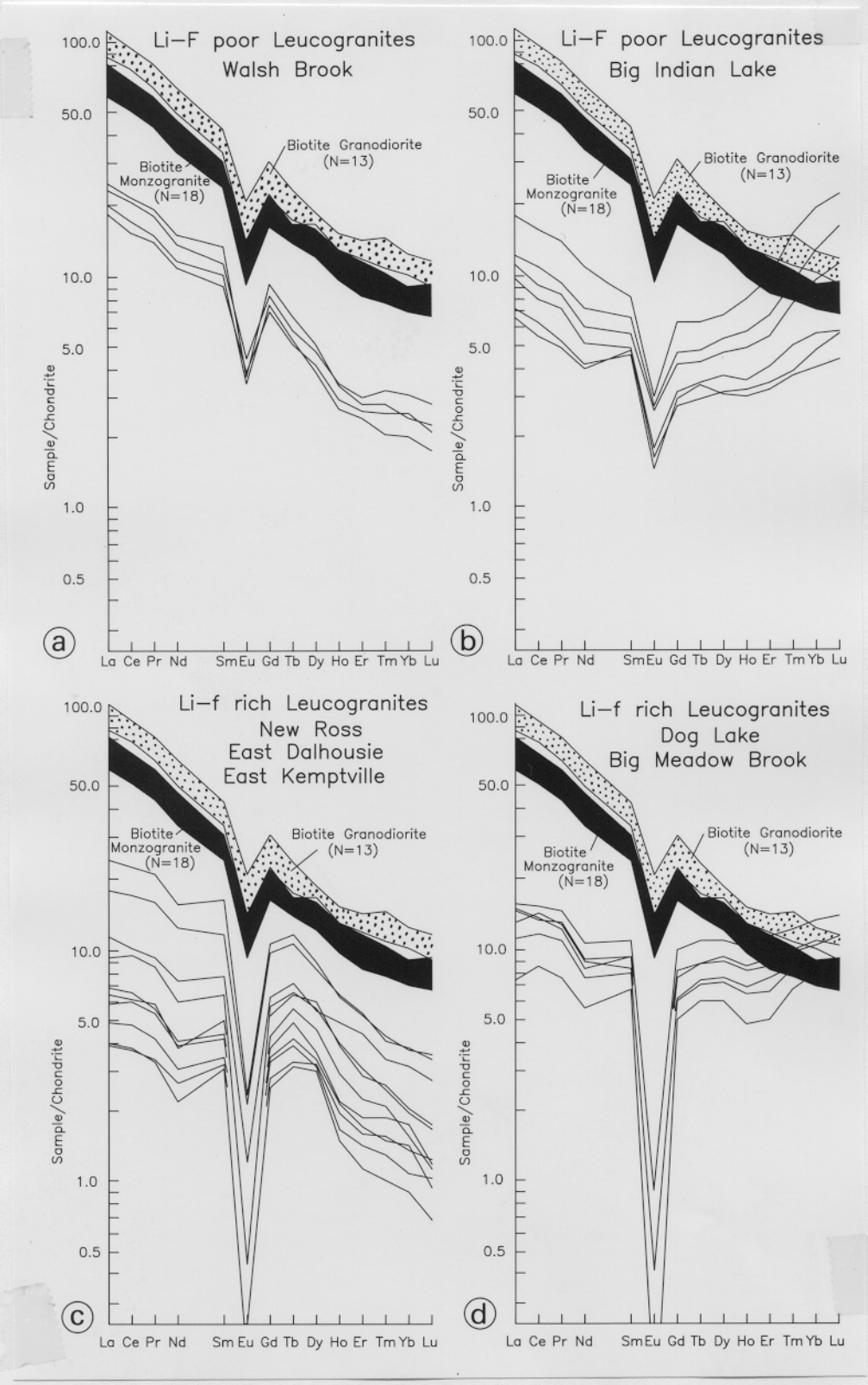

Figure 5.14 Rare earth element (REE) plots for muscovite leucogranites (MLG) from the South Mountain Batholith. See text for discussion.

compared to granodiorite, and have "Wing" shaped REE spectra (Fig. 5.14d) with very low values of Gd/Lu_N (0.71) and La/Lu_N (1.30).

Previous studies of leucogranitic rocks in the batholith have concluded, largely based on geochemical parameters, that these rocks have undergone extensive fluid/melt and/or fluid/rock interaction (Kontak et al., 1988; MacDonald and Clarke, 1991; Clarke et al., 1993; Chatterjee and MacDonald, 1993). It is therefore reasonable to conclude that the diverse trace and RE element compositions of leucogranites may be a result of varying degrees of fluid-rock interaction. However, some leucogranite REE spectra mirror the patterns of the host pluton, as shown by the REE spectra for muscovite-biotite monzogranites in the previous section. Perhaps the best example of this is the "flat" REE spectra in samples from the Davis Lake leucogranite that closely resembles the spectra of the nearby Solomon Lake muscovite-biotite monzogranite and strongly contrasts the spectra for both the leucogranite units and the Sherwood Muscovite-biotite monzogranite from the New Ross pluton. Therefore the observed RE, major and trace element and trace element geochemistry of leucogranites are likely as a result of a combination of crystal/melt processes in the rocks of the host pluton and late-stage fluid alteration and/or metasomatism. Whatever the exact explanation for the trace and RE element compositions in leucogranite units the most important observation is that most leucogranite units displays unique, and consistent, chemical characteristics. The wide range of F, Li, Rb, Ta and other "incompatible" elements reveals wide ranges in the degree of "specialization" as defined by Tischendorf (1977). In fact,

some leucogranites are "non-specialized". Therefore, the various leucogranites presumably have varying potential for the generation of mineral deposits. It should be noted that the East Kemptville leucogranite (Kontak, 1990), which is host to the East Kemptville Sn-Cu-Zn-Ag deposit, has some of the highest concentrations of "incompatible" elements (e.g. F and Rb) in the entire batholith. The economic implications of leucogranite composition are further discussed in Chapter 9.

5.2.4 Geochemistry of Aplite Dykes

As previously noted, aplite and pegmatite dykes were observed to intrude all rock types of both Stage I and II plutons but generally constitute only a minor proportion of most map units (e.g. $<<1\%$). In general, dyke rock are more leucocratic than their host rocks, some being leucogranites *sensu stricto* (i.e. $<2\%$ combined mafic minerals). Based on these factors dyke rocks have traditionally been considered to have highly "evolved" composition although few comprehensive geochemical studies have been conducted. A detailed study of a series of aplite and aplitic portions of pegmatite-bearing dykes, from an outcrop in the Halifax Pluton, was

undertaken as part of this study, as previously indicated in Chapter 4. Eight aplite samples were submitted for major, trace and RE element analysis.

The eight aplite samples have wide variations for most major element concentrations, including 71.23-76.00% SiO_2, 0.93-2.12% Fe_2O_3, 0.10-0.60% CaO, 0.42-1.07% MgO, 0.05-0.29% TiO_2 (Table 5.4). These compositional ranges are similar to the entire range for Stage II plutons as listed in Table 5.2. Concentrations of Na_2O (2.42-3.41%) are significantly lower than the average compositions for the major rock types in the batholith whereas K_2O values ($\leq$6.00%) far exceed the average concentrations in most of the batholith as shown in Figure 5.15. Concentrations of several "compatible" trace elements, including Ba (58-646 ppm), Sr (14-117 ppm), Zr (27-141 ppm), La (2-36 ppm) and Sc (0.6-4.9 ppm), approximate the entire compositional range for the batholith as shown in Figures 5.15). Concentrations of "incompatible" elements are very low with some elements having lower concentrations than biotite granodiorite, the least evolved rock type, as shown in Figure 5.15.

Rare Earth Element (REE) analyses for the eight aplites from a single outcrop are given in Table 5.5. Chondrite-normalized plots were calculated for the REE using the chondrite abundances of Enensen et al. (1978) and are displayed in Figures 5.16.a,b. A sample of the biotite monzogranite host rock has been included for comparison. Several observations can be made regarding the REE data. First, there are very large variations in the overall concentrations of the REE and the shape of the spectra from those that approximate the host monzogranite (e.g. 103-A1) to highly depleted spectra (e.g. 103-A2, -A3, -A8, Group II aplites in Figure 5.15).

All samples in Figure 5.16a have lower $\sum$REE but similar La/Sm and Gd/Lu as the host monzogranite. These samples, along with 103-A1, constitute Group I aplites in Figure 5.15. Conversely, the samples plotted in Figure 5.16b have very "flat" to "wing shaped" REE spectra

Table 5.4. Major and trace element contents of aplites from outcrop of Sandy Lake Biotite Monzogranite, Halifax Pluton.

Sample #	103-A1	103-A2	103-A3	103-A4	103-A5	103-A6	103-A8	103-A9
Major Oxides								
SiO_2	71.27	73.50	71.23	73.75	75.79	76.00	73.26	74.73
Al_2O_3	14.57	14.14	15.15	14.49	13.45	13.97	14.42	14.19
$Fe_2O_{3(T)}$	2.12	1.39	1.18	1.56	0.93	0.95	1.45	0.78
CaO	0.60	0.32	0.32	0.29	0.10	0.10	0.28	0.17
MgO	1.07	0.68	0.68	0.62	0.48	0.42	0.64	0.58
Na_2O	2.77	2.42	2.46	3.10	2.71	3.41	3.04	2.71
K_2O	5.75	6.00	6.77	4.53	5.50	4.59	4.74	4.93
TiO_2	0.29	0.15	0.13	0.13	0.05	0.03	0.14	0.02
MnO	0.04	0.05	0.05	0.07	0.04	0.06	0.07	0.05
P_2O_5	0.32	0.25	0.34	0.19	0.15	0.25	0.28	0.17
LOI	0.30	0.40	0.70	0.40	0.10	0.40	0.50	0.60
Total	99.11	99.30	99.03	99.15	99.31	100.18	98.82	98.93
Trace Elements								
Ba	646	327	574	294	62	58	248	115
Rb	179	169	188	214	170	237	218	153
Sr	117	65	95	51	19	14	50	32
Zr	141	57	66	138	34	25	70	27
Nb	8	5	<5	<5	<5	<5	7	<5
V	12	8	<5	7	<5	<5	<5	<5
Y	16	9	9	31	9	<5	8	5
Ga	17	15	16	16	17	21	17	17
Zn	41	21	21	28	15	15	28	11
Sc	4.9	3.6	2.8	4.4	1.5	1.1	3.4	0.6
Hf	4	2	3	4	1	<1	1	<1
Th	12.0	5.4	4.3	9.3	3.1	1.3	6.3	1.7
U	4.3	5.5	5.3	13.0	6.7	6.8	3.5	3.8
Ta	<0.5	1.4	1.1	1.4	0.5	1.1	2.1	<0.5
Cs	6.2	3.7	4.6	8.1	4.1	19.0	17.0	5.8
W	<1	<1	<1	<1	<1	1	1	<1
Sn	4	13	20	21	14	22	21	19
Li	39	26	25	64	68	49	68	37
F	350	252	269	160	63	124	273	50
B	15	15	26	32	14	20	40	27
La	36	12	12	18	3	2	14	3
K/Rb	266	294	298	175	268	160	180	267

Table 5.5. Rare Earth Element (REE) analytical results for aplites and host biotite monzogranite, Halifax Pluton.

Sample # Rock Type	103-A1 APLI	103-A2 APLI	103-A3 APLI	103-A4 APLI	103-A5 APLI	103-A6 APLI	103-A8 APLI	103-A9 APLI	ASPO-2 BMG
Element									
La	26.40	10.25	9.99	14.87	2.49	1.74	11.43	1.86	22.66
Ce	60.72	23.49	23.33	32.92	5.72	3.69	25.51	4.16	50.29
Pr	7.44	2.90	2.86	3.92	0.73	0.50	3.18	0.52	6.16
Nd	26.69	11.84	10.83	14.73	2.84	1.82	12.53	1.90	23.52
Sm	7.18	3.17	3.17	3.93	1.11	1.04	3.48	0.71	5.23
Eu	0.82	0.44	0.64	0.34	0.10	0.07	0.35	0.19	0.74
Gd	5.82	2.65	3.15	4.10	1.15	0.80	2.95	0.87	4.66
Tb	0.71	0.40	0.49	0.72	0.25	0.17	0.45	0.21	0.80
Py	3.80	2.38	2.92	5.06	1.97	1.32	2.41	1.56	4.97
Ho	0.56	0.38	0.42	1.03	0.40	0.25	0.41	0.28	0.91
Er	1.51	1.03	1.11	3.30	1.30	0.77	1.02	0.88	2.60
Tm	0.20	0.15	0.16	0.54	0.19	0.17	0.16	0.16	0.37
Yb	1.27	0.99	0.97	3.73	1.48	1.33	1.17	1.26	2.24
Lu	0.16	0.13	0.11	0.55	0.22	0.19	0.17	0.18	0.33

Rock Type - APLI - Aplite; BMG - biotite monzogranite

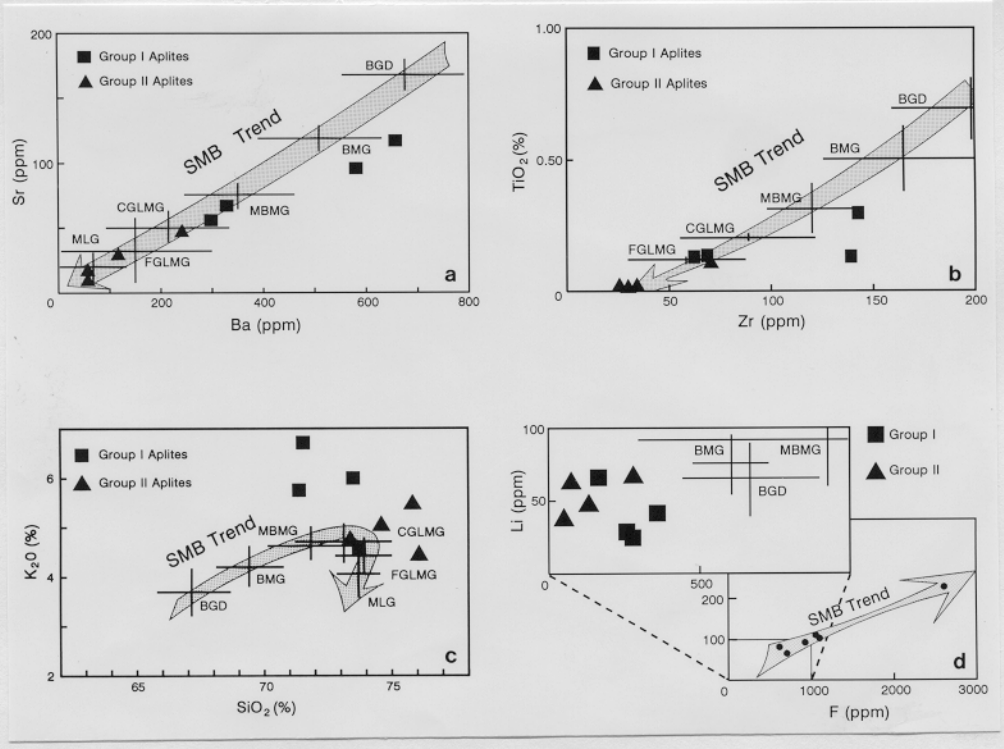

Figure 5.15 Bivariate plots of Sr vs Ba; TiO_2 vs Zr; K_2O vs SiO_2; and Li vs F for 8 aplite samples from the Halifax Pluton. Overall compositional trends for the SMB have been plotted for comparison. See text for discussion.

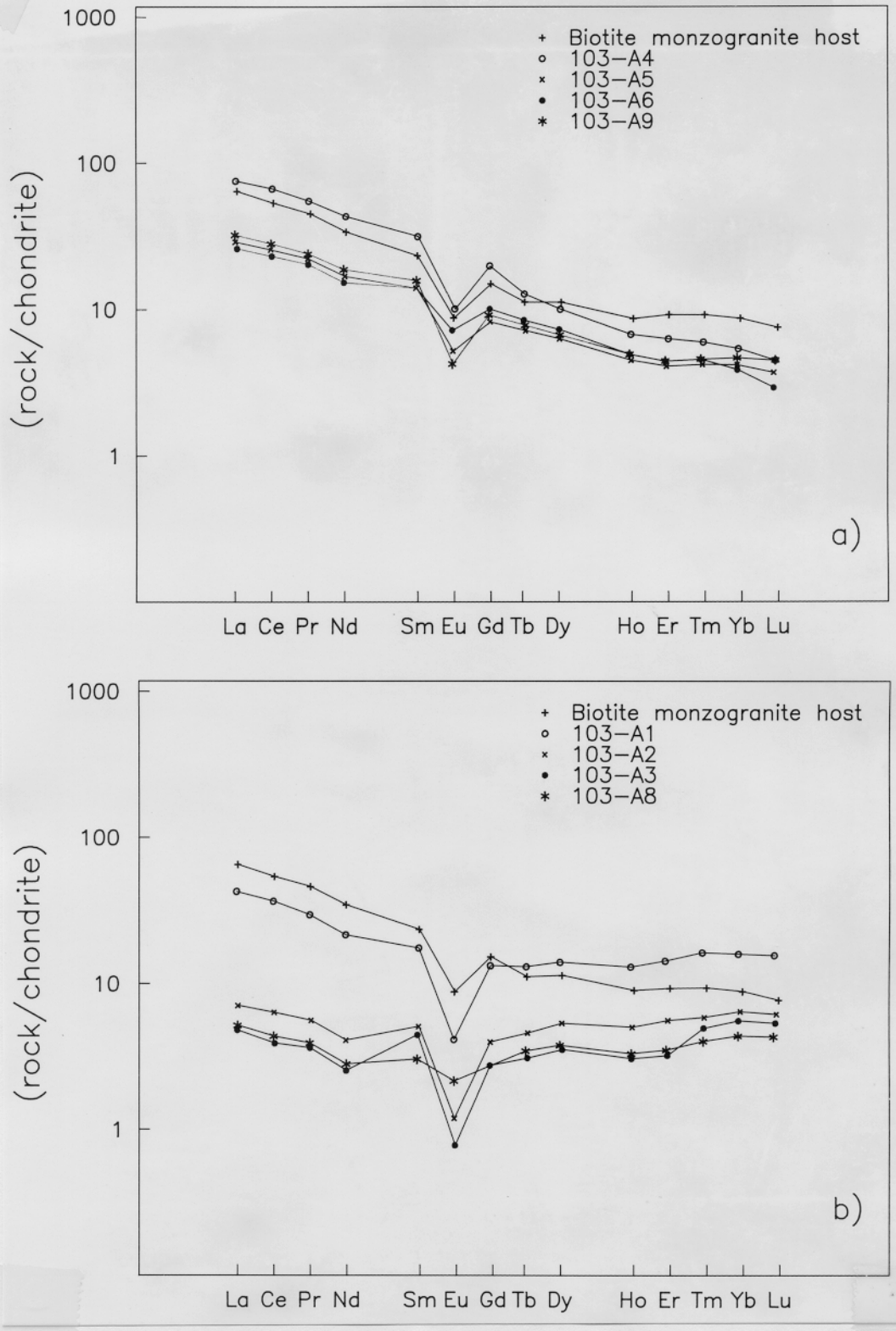

Figure 5.16 Rare earth element (REE) plots for 8 aplite samples from the Halifax Pluton. See text for discussion.

with very low (La/Sm) and Gd/Lu, in fact these aplites have positive slopes for the "heavy" REE (i.e. Gd to Lu) that are unlike the REE spectra of the biotite monzogranite host rock.

Several observations can be made on the basis of the above geochemistry. First, all of the major, trace and REE data demonstrate large compositional variations in aplite and aplite/pegmatite dykes from a single outcrop in the Halifax Pluton. Sample 103-A1 has the highest modal proportion of biotite in the sample set and has very similar chemical composition to its host biotite monzogranite. In contrast, the more "evolved" dykes (i.e. 103-A5, 103-A6) have very low "compatible" trace elements and REE compared to host rocks. All dykes have low concentrations of "incompatible" elements when compared to average concentrations for the major rock types of the batholith. In fact, none of the examined dykes satisfy the chemical criteria for "specialized" granites (as outlined by Tischendorf, 1977), despite several are classified as leucogranites (i.e. $<2\%$ combined mafic minerals). The presence of two distinct types of REE spectra conflicts with a model for dyke generation that involves fractional crystallization from the monzogranite host. The low levels of "incompatible" elements may reflect the presence of contemporaneous pegmatites in the outcrop. It is probable that some elements including F and Li were selectively partitioned into the volatile-rich pegmatite melt during second or resurgent boiling (Hyndman, 1972) which would explain the low levels of these elements in the aplites. It is also possible that some of the REE distribution may be attributed to fluid-stripping within the granite melt, as noted by Muecke and Clarke (1981), although this is highly speculative based on the above data. In summary, the suite of aplite dykes from a single outcrop in the Halifax Pluton has a wide range of compositions. It is not clear whether these observations can be applied to aplite dykes throughout the batholith.

5.2.5 Geochemistry of Mafic Porphyry Rocks

Mafic porphyry rocks were mapped in both Stage I and II plutons throughout the batholith. Mafic porphyry units typically contain abundant metasedimentary xenoliths and are situated at or near granite/metasedimentary rock contacts, with the exception of those in the Halifax and New Ross Stage II plutons. Mafic porphyry rocks are characterized by a wide range of grain size, texture and modal mineralogy, as previously noted in previous chapters. Most map bodies are small (<1 km^2) and, consequently, only a small number of samples have previously been chemically analyzed (Ham et al., 1989, 1990). A compendium of analyses for mafic porphyry from the entire batholith is given in Table 5.6. It is clear from these data that mafic porphyries have highly variable major and trace element geochemistry.

A mesonormative plot (after LeMaitre, 1989) for the four mafic porphyry bodies is given in Figure 5.17. Two samples that were collected approximately 300 m apart in the Sambro mafic porphyry body from the Halifax Pluton have dissimilar compositions, although both samples plot in the granodiorite field. Sample D12-3059 (70.13% SiO_2; 2.50% Fe_2O_3; 220 ppm Rb; 89 ppm Sr) is very similar in composition to muscovite-biotite monzogranite from the Halifax Pluton (71.07% SiO_2; 2.83% Fe_2O_3; 242 ppm Rb; 92 ppm Sr) whereas sample D12-3061 (67.94% SiO_2; 3.98% Fe_2O_3; 135 ppm Rb; 151 ppm Sr) resembles the composition of biotite granodiorite from the same pluton (67.79% SiO_2; 4.10% Fe_2O_3; 164 ppm Rb; 171 ppm Sr). Four samples from the Lequille mafic porphyry (Corey and Horne, 1994b) have uniform compositions (63.27-64.47% SiO_2; 6.16-6.23% Fe_2O_3; 135-145 ppm Rb; 175-189 ppm Sr) and plot along the granodiorite/monzogranite join on LeMaitre's (1989) plot. Both samples from the mafic porphyry body near Big St. Margaret's Bay (Ham and Horne, 1987) have similar compositions and plot

Table 5.6 Major and trace element analyses and normative mineralogy for mafic porphyry bodies from the SMB

SAMPLE	D05-3059	D05-3060	A16-3046	A16-3047	A11-2270-C	LQ-92-1	LQ-92-2	LQ-92-3	A10-3052
Pluton	HP	HP	NRP	NRP	SGP	SGP	SGP	SGP	STP
	Major Elements (wt %)								
SIO2	70.13	67.94	69.50	70.01	63.82	64.47	63.91	63.27	67.22
AL2O3	14.65	14.84	14.47	14.28	16.09	16.08	16.09	16.39	15.36
FE2O3	2.50	3.98	3.68	3.46	6.36	6.23	6.11	6.16	4.37
CAO	1.21	2.32	0.87	0.97	1.74	1.94	1.95	2.1	1.26
MGO	3.60	2.12	1.64	1.50	2.12	1.62	1.67	1.64	1.78
NA2O	3.63	4.56	3.43	3.93	3.14	2.91	2.86	2.91	3.21
K2O	4.14	3.49	4.12	4.35	3.47	3.65	3.67	3.72	4.25
TIO2	0.29	0.56	0.51	0.47	0.85	0.84	0.84	0.82	0.87
P2O5	0.20	0.20	0.21	0.21	0.23	0.23	0.23	0.23	0.21
MNO	0.07	0.08	0.06	0.07	0.17	0.13	0.12	0.13	0.07
H2O	0.50	0.70	0.80	0.70	1.20	0.9	1.1	0.9	0.67
	Normative Mineralogy								
Q	25.65	20.57	30.51	26.97	26.56	n.d.	n.d.	n.d.	27.90
OR	24.39	20.62	24.74	25.92	20.95	n.d.	n.d.	n.d.	25.50
AB	30.58	38.55	29.47	33.50	27.11	n.d.	n.d.	n.d.	27.54
AN	4.67	9.70	2.99	3.46	7.27	n.d.	n.d.	n.d.	4.95
C	2.46	0.00	3.34	1.86	4.65	n.d.	n.d.	n.d.	3.74
EN	8.93	5.10	4.15	3.76	5.39	n.d.	n.d.	n.d.	4.50
IL	0.15	0.17	0.13	0.15	0.37	n.d.	n.d.	n.d.	0.15
HM	2.49	3.98	3.74	3.49	6.49	n.d.	n.d.	n.d.	4.43
RU	0.21	0.47	0.45	0.39	0.67	n.d.	n.d.	n.d.	0.80
AP	0.46	0.46	0.49	0.49	0.54	n.d.	n.d.	n.d.	0.49
A/CNK	1.16	0.96	1.24	1.10	1.33	n.d.	n.d.	n.d.	1.26
TTDI	80.62	79.74	84.72	86.39	74.61	n.d.	n.d.	n.d.	80.94
Col. Ind.	11.57	9.63	8.01	7.40	12.25	n.d.	n.d.	n.d.	9.08
	Trace Elements (ppm)								
Ba	262	446	483	467	744	756	755	694	888
Rb	220	182	210	217	135	145	141	144	153
Sr	89	151	118	99	181	189	175	175	132
Zr	90	148	160	152	294	282	282	287	222
Nb	10	12	12	12	14	15	15	14	9
V	20	50	40	36	97	84	76	83	69
Y	22	22	25	25	46	46	43	48	32
Ga	19	20	26	22	17	21	22	23	19
Cu	0	4	5	0	7	19	20	17	8
Zn	43	74	73	57	790	94	79	81	70
Hf	3	3	4	4	8	7	7	7	6
Ta	1.1	1.6	1.5	1.5	1.4	1.5	0.9	1.2	1.1
Sc	8.8	5.5	8.5	7.9	14.0	16	16	17	9.4
La	27	16	31	29	45	51	50	48	38
Th	12.0	8.0	11.0	11.0	15.0	15	15	14	16.0
U	3.6	4.4	4.3	2.9	3.6	3.4	3.6	3.4	4.1
Li	95	94	73	73	66	62	59	51	31
F	710	590	640	690	674	641	611	661	660
As	6.1	2.4	4.3	1.2	9.0	8.4	8.3	7.4	8.2
Sn	15	12	11	10	0	7	2	2	2
W	1	1	1	1	0	0.5	0.5	0.5	0

n.d. - not determined

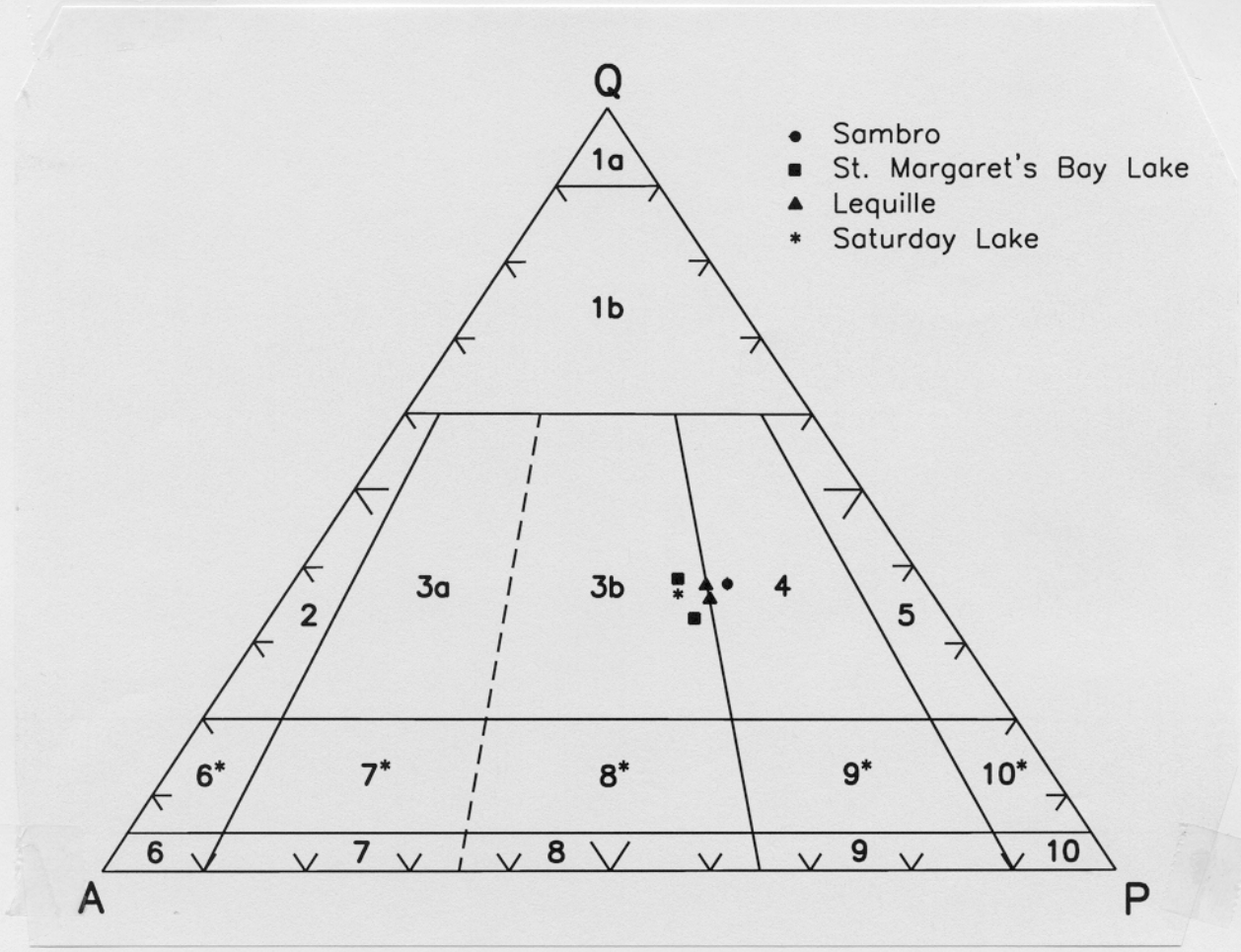

Figure 5.17 Ternary plot of average CIPW normative data for mafic porphyry rocks from the entire SMB (fields after LeMaitre, 1989). See text for discussion.

in the monzogranite field of Lemaitre (1989).

In light of the above results a geochemical study of the Boot Lake granodiorite/mafic porphyry body (MacDonald and Ham, 1992) was undertaken. A suite of 19 samples was collected and analyzed for major and trace elements by the methods outlined in Section 5.1. Analytical results are given in Table 5.7. Rocks designated "hybrid" are mafic porphyry with abundant garnet±pyrite±arsenopyrite that form "swirling" or wispy bands in Halifax Formation slate with ptygmatic folds. Rocks designated "garnet-bearing mafic porphyry" have common to abundant orange-red garnet with common pyrite and arsenopyrite and are situated adjacent to large blocks

Table 5.7 Major and trace element analyses for the Boot Lake unit (after MacDonald and Ham, 1992)

Rock Type	HR	HR	HR	GMP	GMP	BRGD	BRGD	BRGD	BRGD	BRGD	BRGD
Sample	A15-80-8	A15-80-9	A15-0087	A15-80-5	A15-80-6	A15-0080	A15-0081	A15-80-7	A15-80-10	A15-80-11	A15-80-13
Major Elements (wt. %)											
SiO2	69.48	65.34	60.85	65.96	62.92	64.72	65.36	64.45	62.67	62.24	65.01
Al2O3	16.01	17.51	18.70	16.72	17.08	16.63	15.33	15.95	16.47	16.19	16.58
Fe2O3	4.96	5.88	6.36	5.89	6.64	4.89	5.98	6.16	7.50	7.64	5.09
MgO	1.04	1.59	0.96	1.81	1.93	3.07	2.38	1.58	1.74	1.80	1.56
CaO	1.68	1.12	2.04	2.30	2.50	2.13	1.80	2.22	3.04	3.09	3.21
Na2O	2.75	2.38	2.13	2.79	2.71	3.98	3.33	3.18	3.16	3.21	3.71
K2O	1.50	3.19	4.48	2.37	3.23	2.64	3.46	3.06	3.20	2.87	2.73
TiO2	0.68	0.80	0.88	0.88	0.99	0.77	0.82	0.85	1.06	1.05	0.79
MnO	0.08	0.14	0.16	0.42	0.44	0.28	0.24	0.11	0.14	0.13	0.07
P2O5	0.24	0.18	0.18	0.11	0.22	0.08	0.11	0.32	0.32	0.31	0.32
LOI	1.80	2.00	2.48	0.50	1.10	0.40	0.41	0.80	0.30	0.60	0.20
Trace Elements (ppm)											
Ba	311	626	1101	533	817	562	819	657	1040	939	531
Rb	81	126	164	116	161	141	130	138	131	129	148
Sr	195	135	166	187	208	209	179	180	206	208	202
Zr	257	218	220	246	260	162	286	280	333	338	163
Nb	14	15	15	13	17	12	15	17	20	19	11
V	48	91	106	78	95	61	65	68	82	85	58
Y	47	39	43	43	49	27	48	60	55	49	24
Ga	20	21	25	20	23	22	21	20	20	21	19
Cu	15	28	35	12	19	28	13	10	19	14	28
Zn	72	102	98	75	102	83	84	63	88	89	79
Hf	8	7	7	7	7	5	10	8	10	10	4
Ta	1.4	1.5	1.3	1.2	1.3	1.0	1.4	1.3	1.5	1.5	1.2
Sc	23.7	22.7	15.0	20.6	24.2	13.0	16.0	24.0	24.6	23.7	16.0
La	53	51	51	54	59	25	48	53	63	65	24
Th	18.0	16.0	15.0	16.0	17.0	8.4	15.0	15.0	18.0	19.0	7.2
U	3.2	5.1	4.2	3.4	3.8	4.2	3.4	3.4	1.8	1.7	4.1
Li	45	46	69	40	23	65	51	52	47	58	50
F	372	366	450	557	873	635	710	740	600	601	477
As	3.5	11.0	18.0	28.0	24.0	1.7	3.8	11.0	2.0	2.6	1.1
Sn	2	2	0	2	2	0	2	8	7	7	2
W	0.5	1	0	1	0.5	0	0	0.5	0.5	1	0.5

Rock Types: HR - hybrid rocks; GMP - garnet-rich mafic porphyry; BRGD - biotite-rich granodiorite; G-FGLMG - garnet-bearing fine-grained leuco-monzogranite BMG - biotite monzogranite; MBMG - muscovite-biotite monzogranite; FGLMG - fine-grained leucomonzogranite.

Symbols

Hybrid Rocks - HR

Garnet-rich mafic porphyry - GMP

Biotite-rich granodiorite - BRGD

Garnet-bearing f-g leucomonzogranite - G-FGLMG

Biotite monzogranite - BMG

Muscovite-biotite monzogranite - MBMG

Fine-grained leucomonzogranite - FGLMG

Rock Type	BRGD	MBMG	MBMG	MBMG	MBMG	G-FGLMG	G-FGLMG	G-FGLMG	BMG	BMG	BMG
Sample	A15-80-18	15-0080-2	A15-80-12	A15-80-14	A15-80-15	A15-80-16	A15-80-17	15-0087-G	A15-116	A15-116-2	A15-116-3
Major Elements (wt. %)											
SiO2	64.98	70.58	70.34	75.05	71.00	71.84	68.91	68.73	68.30	68.77	69.05
Al2O3	15.82	15.30	15.33	13.90	15.09	15.69	16.77	17.01	14.80	14.73	14.39
Fe2O3	6.16	2.25	2.12	0.81	2.13	1.03	0.73	0.76	4.29	4.05	4.28
MgO	1.57	1.33	0.75	0.16	0.67	0.01	0.00	0.89	1.73	1.63	1.59
CaO	2.20	1.37	1.18	1.57	1.39	0.74	0.35	0.72	1.45	1.43	1.40
Na2O	3.05	3.99	3.06	2.73	3.28	3.47	2.78	4.42	3.24	3.45	3.36
K2O	3.06	3.95	4.39	3.90	3.93	5.56	8.54	6.02	3.97	4.24	4.23
TiO2	0.87	0.31	0.31	0.11	0.28	0.02	0.03	0.03	0.56	0.53	0.56
MnO	0.11	0.17	0.05	0.02	0.06	0.18	0.15	0.21	0.20	0.19	0.18
P2O5	0.31	0.06	0.23	0.07	0.20	0.22	0.26	0.14	0.09	0.09	0.09
LOI	1.40	0.50	0.60	0.20	0.60	0.60	0.40	0.34	0.40	0.11	0.12
Trace Elements (ppm)											
Ba	687	551	423	1500	323	294	485	394	581	599	625
Rb	139	141	162	96	190	194	331	240	151	172	164
Sr	179	150	135	201	106	57	75	97	133	124	119
Zr	270	97	95	84	73	30	23	43	214	200	211
Nb	17	8	9	<5	9	<5	<5	0	13	12	12
V	67	27	27	<5	24	<5	<5	0	36	41	40
Y	61	16	12	<5	13	7	<5	22	45	43	46
Ga	21	17	17	11	17	15	16	16	18	19	20
Cu	11	0	<5	5	<5	13	23	89	8	9	10
Zn	64	45	33	14	46	11	10	11	60	59	68
Hf	10	3	3	3	2	2	1	2	7	7	6
Ta	1.1	0.6	1.1	0.2	1.4	0.2	0.2	0.0	1.2	1.3	1.0
Sc	26.6	5.7	6.8	2.3	6.9	4.9	4.0	2.9	11.0	10.0	10.0
La	55	21	22	19	16	4	4	24	34	35	34
Th	15.0	10.0	10.0	6.6	8.0	0.6	2.1	15.0	12.0	13.0	12.0
U	3.6	2.7	5.8	2.6	3.5	2.1	2.4	10.0	3.7	4.7	2.8
Li	38	49	32	10	55	11	9	12	57	66	62
F	570	330	260	80	269	93	70	70	725	730	705
As	10.0	0.0	2.5	0.5	0.5	2.5	0.5	1.6	2.1	2.2	3.3
Sn	2	3	2	2	10	9	2	2	0	3	9
W	0.5	0	0.5	0.5	0.5	0.5	0.5	0	2	3	0

Rock Type	BMG	BMG	BMG	BMG	BMG	BMG	BMG	BMG	BMG	FGLMG	FGLMG
Sample	A15-118	A15-120-2	A15-141-2	A14-001	A14-002	A14-002-1	A14-003	A14-008	A14-1030	A15-0142	A14-1040
Major Elements (wt. %)											
SiO2	67.82	67.23	67.46	69.74	68.97	69.28	69.44	69.58	70.22	75.27	76.25
Al2O3	15.06	15.13	15.02	14.79	15.31	14.95	14.71	14.83	14.66	13.36	13.47
Fe2O3	4.35	4.71	4.30	3.70	4.00	4.02	4.47	4.07	3.55	1.47	1.20
MgO	1.44	1.94	1.63	1.35	1.66	1.59	1.72	1.46	1.50	0.28	0.23
CaO	1.80	1.46	1.59	1.39	1.51	1.33	1.68	1.36	1.21	0.75	0.82
Na2O	3.73	3.70	3.88	3.38	2.57	3.24	2.65	3.52	3.48	3.67	3.13
K2O	3.85	3.88	4.09	4.15	4.02	4.20	3.98	4.05	4.27	4.71	4.62
TiO2	0.59	0.62	0.55	0.45	0.51	0.51	0.58	0.50	0.43	0.06	0.06
MnO	0.20	0.19	0.18	0.18	0.20	0.20	0.19	0.18	0.18	0.13	0.16
P2O5	0.09	0.09	0.10	0.09	0.09	0.09	0.09	0.10	0.08	0.07	0.07
LOI	0.52	0.20	0.38	0.70	0.60	0.40	0.10	0.40	0.20	0.13	0.40
Trace Elements (ppm)											
Ba	546	642	643	487	565	606	604	595	519	91	72
Rb	158	151	174	187	172	169	173	175	182	259	276
Sr	127	143	126	119	123	127	134	127	112	16	10
Zr	208	219	207	173	196	202	211	194	186	58	40
Nb	13	12	13	12	11	13	15	14	11	7	7
V	47	51	39	30	33	33	39	30	29	0	0
Y	45	48	43	42	38	42	39	37	41	32	20
Ga	17	21	21	16	16	17	18	16	19	16	16
Cu	11	9	6	0	0	0	0	0	0	0	0
Zn	59	70	67	56	61	66	61	54	56	28	25
Hf	7	8	7	7	8	9	8	7	6	2	2
Ta	1.4	1.3	1.3	1.5	1.2	1.2	1.1	1.2	1.0	1.7	1.3
Sc	12.0	12.0	11.0	7.5	9.1	10.0	9.3	9.0	7.2	3.1	3.1
La	35	38	35	31	35	38	34	34	31	6	4
Th	13.0	13.0	13.0	13.0	13.0	14.0	12.0	12.0	12.0	5.3	3.0
U	3.1	4.5	3.4	3.8	3.5	3.2	3.3	3.7	3.5	3.5	1.6
Li	62	59	63	59	59	53	62	58	62	65	106
F	650	730	735	695	633	570	698	566	628	270	327
As	5.2	13.0	5.0	9.0	2.1	2.1	30.0	2.0	1.5	12.0	8.6
Sn	5	1	0	13	7	2	11	10	5	9	11
W	0	0	0	0	3	1	1	3	1	3	5

Rock Type	FGLMG	FGLMG	FGLMG	FGLMG	FGLMG
Sample	14-C002A	A14-C004	A14-1006	14-1006-1	A14-1007
Major Elements (wt. %)					
SiO2	75.64	76.10	75.38	75.23	75.16
Al2O3	13.62	13.74	13.72	13.53	13.76
Fe2O3	1.30	0.98	1.15	1.30	1.18
MgO	0.24	0.37	0.28	0.22	0.25
CaO	0.77	0.87	0.73	0.87	0.79
Na2O	3.80	3.59	4.31	4.09	3.82
K2O	4.22	3.54	4.19	4.54	4.48
TiO2	0.03	0.04	0.03	0.04	0.04
MnO	0.14	0.14	0.16	0.15	0.12
P2O5	0.06	0.02	0.05	0.07	0.08
LOI	0.40	0.40	0.40	0.40	0.80
Trace Elements (ppm)					
Ba	36	67	123	23	22
Rb	288	213	286	307	283
Sr	13	39	20	12	11
Zr	39	46	45	44	43
Nb	5	7	6	7	8
V	0	16	0	0	0
Y	24	20	20	26	23
Ga	16	19	18	16	18
Cu	0	52	0	0	0
Zn	51	25	36	43	21
Hf	2	1	2	2	2
Ta	1.7	1.7	2.2	1.8	1.8
Sc	2.4	3.5	2.9	3.1	3.2
La	4	5	3	4	4
Th	3.9	4.2	4.3	4.3	4.2
U	7.8	13.0	4.5	4.8	4.8
Li	21	19	21	57	41
F	63	177	160	317	120
As	8.4	22.0	17.0	7.3	17.0
Sn	0	0	0	0	0
W	3	8	11	4	1

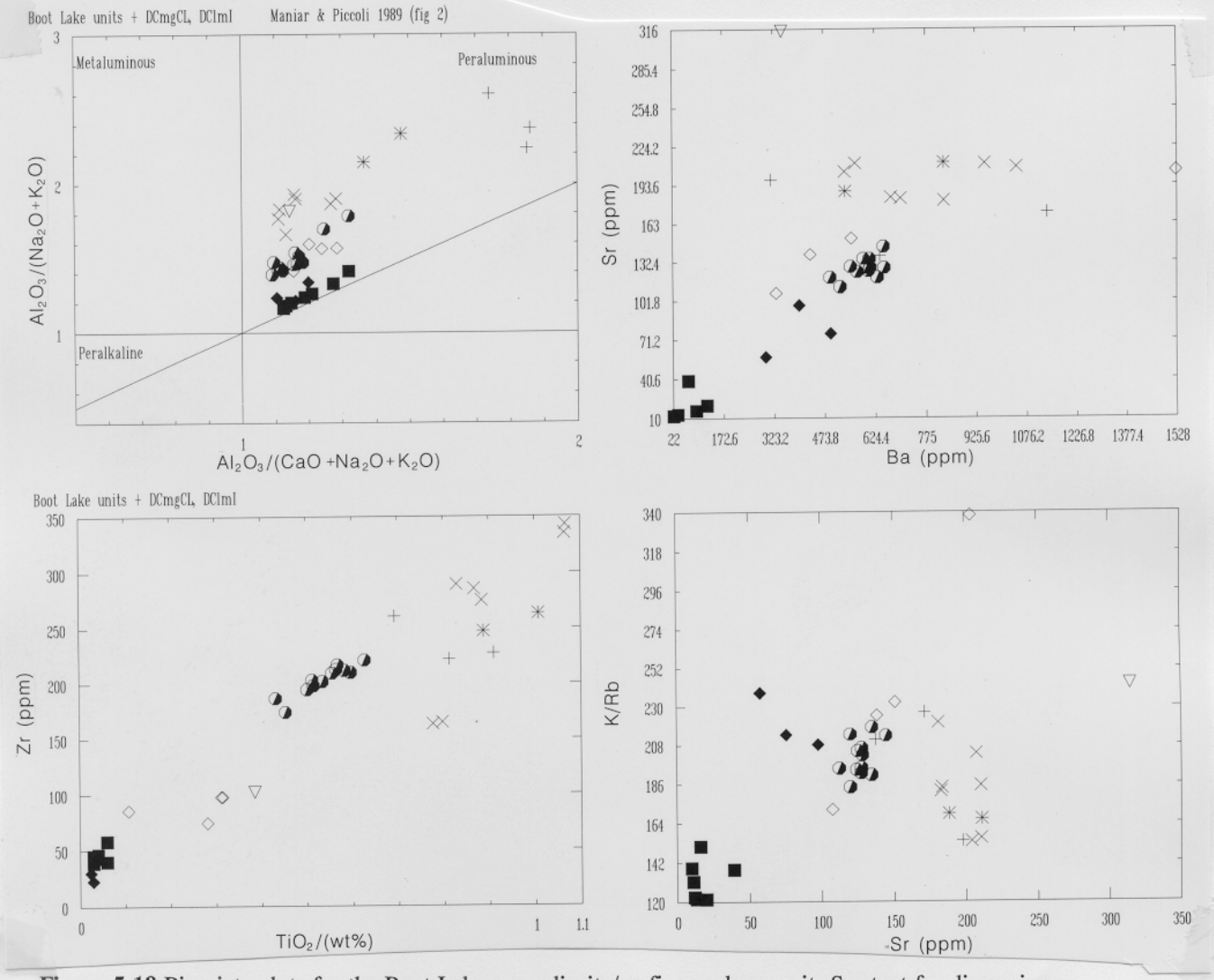

Figure 5.18 Bivariate plots for the Boot Lake granodiorite/mafic porphyry unit. See text for discussion.

of metasedimentary rocks. Rocks designated "biotite-rich granodiorite" are primarily fine- to medium-grained with slightly porphyritic texture with minor modal amounts of quartz and feldspar phenocrysts. These rocks do not have a close spatial association with metasedimentary rocks and have fewer xenoliths than the two previous groups. Several isolated outcrops of muscovite-biotite monzogranite were noted within the Boot Lake unit and a garnet-bearing leucogranite dyke was also noted in the eastern end of the unit. The exact relationship between these rocks and the rest of the unit is unclear, as indicated in Chapter 3.

The sequence of hybrid rocks, garnet-bearing mafic porphyry and biotite-rich granodiorite is marked by large ranges in major element concentrations including 60.85-65.96% SiO_2; 4.89-7.64% Fe_2O_3; 1.12-3.21% CaO; 0.96-3.07% MgO; 0.68-1.06% TiO_2. Samples with the highest SiO_2 and the lowest Fe_2O_3, CaO, MgO and TiO_2 closely resemble average biotite granodiorite of the entire batholith, whereas other samples have the lowest SiO_2 and highest concentrations of ferromagnesian and some "compatible" elements (1101 ppm Ba; 209 ppm Sr; 338 ppm Zr; 26.6 ppm Sc; 65 ppm La) in the entire batholith.

Three possible origins for the Boot Lake mafic porphyry rocks, based primarily on field relations, include: 1) contamination of granodiorite magma via extensive assimilation of Meguma Group metasedimentary rocks; 2) sidewall fractional crystallization and/or cumulate development at margins of granodiorite magma; and 3) partial melting of Meguma Group metasedimentary rocks. The viability of each of these processes can be evaluated using the above geochemical data.

A Shand-type plot (Maniar and Piccoli, 1989) for the Boot Lake data is presented in Figure 5.18 (symbols on pg. 132). Hybrid and garnet-bearing mafic porphyry rocks have very high A/CNK values that are among the highest values reported for the batholith. Highly peraluminous compositions are consistent with a large degree of assimilation of aluminous sedimentary rocks. In contrast, the very high concentrations of some "compatible" elements, as outlined above, are difficult to reconcile by a process of assimilation because the levels of these elements in Halifax Formation slates are in fact lower than the average Cloud Lake biotite monzogranite (pers. comm. A.K. Chatterjee, 1993). Therefore extensive assimilation of Meguma Group rocks by the Cloud Lake magma would actually "dilute" the levels of these elements in the resulting rocks.

MacDonald and Horne (1988) evoked a process of sidewall fractional crystallization to

explain the smooth compositional "trends" and formation of biotite granodiorite along the margins of the Halifax Pluton. Bivariate plots of Sr versus Ba, Zr versus TiO_2 and K/Rb versus Sr for the Boot Lake and related samples from Table 5.7 are given in Figures 5.18b to d. It is apparent in all plots that the Cloud Lake biotite monzogranite and Inglisville fine-grained leucomonzogranite form a cohesive, and continuous, sequence whereas the rocks of the Boot Lake unit plot well off this trend, in contrast to the data of MacDonald and Horne (1988). However, Corey (1992) has documented biotite+apatite- and plagioclase-rich cumulate phases within the Big Indian pluton. Corey also described biotite-rich granodiorite rocks that were interpreted as forming from "cumulate" processes. Geochemical analyses from this granodiorite (unpubl. data M.C. Corey) indicated values of most major and trace elements (e.g. 4.89% Fe_2O_3; 3.29% CaO; 1045 ppm Ba; 174 ppm Rb; 209 ppm Sr; 224 ppm Zr) that are remarkably similar to the biotite-rich hybrid, mafic porphyry and granodiorite rocks of the Boot Lake body. This observation suggests that cumulate processes could be responsible, at least in part, for the formation of the Boot Lake mafic porphyry rocks.

It is difficult to estimate the plausibility of partial melting of Meguma Group rocks for the formation of Boot Lake rocks using only the major and trace element geochemical data. Certainly if the hybrid and mafic porphyry rocks represent melanosomes from partially developed migmatites, the high concentrations of "compatible" elements can be explained by the preferential accumulation of ferromagnesian minerals (pers. comm. A.K. Chatterjee, 1993). A more definitive evaluation would require radiogenic and stable isotopic data which would establish the relative contribution of both granite and metasediment sources.

5.4 Summary

This study represents the most comprehensive lithogeochemical study of the South Mountain Batholith to date. The suite of 597 samples characterize the entire range of compositions from the least evolved biotite granodiorite and mafic porphyry to the most evolved leucogranite and hydrothermally altered rocks associated with post-magmatic mineralization. In addition, the geographic distribution of samples provides, for the first time, insight into the internal geochemical variation of plutons.

Perhaps the most striking feature of the geochemistry of the batholith is the overall similarity in composition throughout the batholith. All rocks are peraluminous (i.e. molecular $Al_2O_3/(CaO+K_2O+Na_2O) > 1$) and have relatively high SiO_2 and low CaO with ranges from 67.12% (SD-1.73) and 1.94% (SD-0.46), respectively, in granodiorite to 73.62% (SD-0.89) and 0.39 (SD-0.14), respectively, in leucogranite rocks. The major element chemistry and normative composition of the major rock types indicates a progression from least evolved biotite granodiorite to most evolved leucogranite that reflects the petrographic features of the different rock types. This sequence is marked by systematic decreases in TiO_2, Fe_2O_3, MnO, MgO, CaO, K/Rb and normative anorthite, enstatite, ilmenite, hematite, rutile and colour index and increases in SiO_2, normative quartz, A/CNK and Thornton-Tuttle differentiation index. The concentration of P_2O_5 is generally consistent from granodiorite to fine-grained leucomonzogranite with a sudden increase in leucogranite units. This sequence is also marked by systematic decreases in several compatible trace elements (i.e. Ba, Sr, Zr, V, Hf, Sc and La) and increases in several incompatible trace elements (i.e. Rb, Ta, U, Li, F, Sn and W).

Despite the overall compositional similarities throughout the batholith, it is possible to

distinguish among individual plutons as seen in the Harker variation diagrams of Figures 5.1 and 5.2 and discussed in Section 5.2.3. It is apparent from these plots that the overall concentrations of many elements, and in some cases the slopes of regression lines, vary significantly among the Stage I and II plutons. These data indicate the batholith formed by the coalescence of discrete plutons, in contrast to earlier studies that proposed the entire batholith formed from a single parental magma.

Perhaps one of the most important implications of the geochemical data is the delineation of cryptic normal and reverse compositional zoning in both Stage I and II plutons (MacDonald and Horne, 1988; Horne et al., 1989; MacDonald et al., 1992). The establishment of zoning patterns in the batholith will provide a framework for future work, including mineral exploration.

Geochemical data have also revealed large geochemical ranges in some units, including some with somewhat restricted modal mineralogical variation (e.g. Davis Lake Leucomonzogranite). Large compositional variation in the mafic porphyry bodies may reflect varying degrees of assimilation or wall-rock interaction as evidenced by the very high A/CNK values. Lithogeochemical composition of aplite dykes may also vary significantly as seen in a single outcrop in the Halifax Pluton where dyke rock compositions approximated the entire range for the rest of the batholith. Cryptic REE variations in several rock suites from the batholith merit further work.

In short, the geochemical data generated during the SMB project has yielded new insights into the composition of the batholith and provides an excellent framework for future work.